

UNITED STATES DEPARTMENT OF THE INTERIOR

GEOLOGICAL SURVEY

PRELIMINARY REPORT ON HIGH-FREQUENCY
NEAR-SOURCE RECORDINGS AT PERMANENTE ROCK QUARRY
IN CUPERTINO, CALIFORNIA

compiled and edited by

Chris Dietel¹

OPEN-FILE REPORT 86-330

This report is preliminary and has not been reviewed for conformity with the U.S. Geological Survey editorial standards and stratigraphic nomenclature.

¹Menlo Park, California

1986

CONTENTS

	Page No.
ABSTRACT	1
INTRODUCTION	
C. Dietel.....	1
GENERAL DESCRIPTION OF RECORDING SYSTEM	
G. Jensen, J. Gibbs, R. Borchardt, J. VanSchaack, J. Sena, C. Dietel, E. Sembera, G. Maxwell	1
FIELD DEPLOYMENT	
C. Dietel, J. Gibbs, E. Sembera, J. Sena.....	4
DESCRIPTION OF DATA PLOTS	
C. Dietel.....	6
PRELIMINARY ANALYSIS	
C. Dietel.....	7

ABSTRACT

High-quality digital recordings of two quarry shots were obtained along linear arrays to investigate the efficiency of quarry blasts in the generation of high-frequency seismic energy. Six portable digital systems were deployed at distances from 90 to 2250 meters from shot points. Stations closest to the shot points recorded 3 components of acceleration at 400 samples/second/channel. Furthest stations recorded 3 components of velocity at 400 samples/second/channel, and intermediate stations recorded both acceleration and velocity at 200 samples/second/channel. The recordings show that seismic energy up to 100 Hz was well recorded above seismic background noise out to distances of 2 km. This report provides a description of the Permanente Rock Quarry experiment, instrumentation, data set and preliminary interpretation of results.

INTRODUCTION

The Permanente Rock Quarry is a large circular quarry excavation in hard limestones located in the foothills of Cupertino, California. It has provided an excellent opportunity for a small-scale preliminary study of seismic characteristics of waveforms originating from subsurface explosions. The purpose of the experiment was to obtain high-quality digital recordings of ground motion from close quarry blasts producing high-frequency seismic signals. This study confirms the need for a larger-scaled experiment which will show the capability of recording seismic data which differentiates between small nuclear blasts and other seismic signals.

GENERAL DESCRIPTION OF RECORDING SYSTEM

The portable digital data acquisition system used for the experiments was developed by the U.S. Geological Survey for use in a wide variety of both active and passive experiments. The microcomputer-based system was developed in order that the system could be easily configured in the field to record signals for a variety of different experiments, including studies of strong motion, structural response, source mechanisms, and wave propagation studies of aftershock sequences, crustal structure, teleseismic earth structure, near-surface seismic structure, earth tidal strains, free oscillations and a variety of wave

propagation studies such as those described in this report. Versatility in system application is achieved by isolation of the appropriate data acquisition functions on hardware modules controlled by a central microcomputer via a general computer bus. CMOS hardware components are utilized to reduce quiescent power consumption to less than 2 watts for use of the system as either a portable recorder in remote locations or in an observatory setting with inexpensive backup power sources. Some GEOS instruments at Permanente Rock Quarry were deployed with either a three-component velocity sensor or a three-component force-balance accelerometer, while others used both.

The signal conditioning module for the GEOS is configured with six input channels, selectable under software control, to permit acquisition of seismic signals ranging in amplitude from a few nanometers of seismic background noise to 2 g in acceleration for ground motions near large events. The analog-to-digital conversion module is equipped with a 16-bit CMOS analog-to-digital converter which affords 96 dB of linear dynamic range or signal resolution; this, together with two sets of sensors, implies an effective system dynamic range of about 180 dB. A data buffer with direct memory access capabilities allows for maximum throughput rates of 1200 sps. With sampling rates selectable under software control as any integral quotient of 1200, broad and variable system bandwidth ranging from $(10^{-5} - 5 \times 10^2 \text{ Hz})$ is achieved for use of recorders with a wide variety of sensor types.

Modern high-density, (1600–6400 bpi) compact tape cartridges offer large data storage capacities (2.5–25 Mbyte) in ANSI standard format, to facilitate data accessibility via minicomputer systems. Read capabilities of cartridge tape recorders when fully utilized will permit recording parameters and system operational software to be changed automatically. Expansion of solid state data memory will allow systems equipped with modems to transmit data via telecommunications to a central data processing laboratory. Microcomputer control of time-standard provides capability to synchronize the internal clock to an internal WWVB receiver, external master clock, or conventional digital clocks. Convenient system set-up and flexibility to modify the system in the field for a wide variety of applications is achieved using a 32-character alphanumeric display under control of the microcomputer. English-language messages to operator executed in an interactive mode, reduce operator

field set-up errors. A complete record of recording system parameters is recorded on each tape together with calibration signals for both the sensors and the recorders. These records assure rapid and accurate interpretation of signals, both in the field and in the laboratory.

Flexibility to modify the system to incorporate future improvements in technology is achieved using a ringed software architecture and modular hardware components. Incorporation of new hardware modules is accomplished in a straightforward manner by replacing appropriate module and corresponding segments of controlling software. The flexibility afforded by microcomputer technology to modify the system for specialized applications and to incorporate changes in technology allows seismic signals as detectable by a wide variety of sensors to be recorded over a broad band of frequencies with high resolution.

The system response designed for strong-motion and aftershock applications of the GEOS was intended to allow large-amplitude near-source signals of 1–10 Hz as detected by a force-balanced accelerometer (FBA) to be recorded on scale, while at the same time permitting much smaller-amplitude high-frequency signals (50–100 Hz) as might be detected on FBA's or velocity transducers to be recorded with high signal resolution. With digitization rates and anti-aliasing filters, selectable under software control, the design system response allows signals ranging from essentially DC to 500 Hz to be recorded at high resolution without aliasing. Gain settings, selectable under software control, allow two sets of three-component data, ranging in amplitude over 180 dB, to be recorded simultaneously.

General Description of Data Playback System

The read and write capabilities of the mass-storage module together with the D/A conversion module permits the GEOS to be used as an analog as well as digital (via RS-232) playback system in the field. Visual inspection of digitally recorded data is useful for determining instrument performance, evaluation of recording parameters, evaluation of environmental factors (*e.g.*, local noise sources, etc.). RS-232 capabilities of data playback unit and ANSI-standard tape cartridges permit playback of digital time series on minicomputer systems in the field or laboratory. Digital playback of data is generally performed using an ANSI-standard serpentine tape reader as a peripheral to minicomputer

systems in the laboratory. Deployment of minicomputer digital playback systems in the field is generally most feasible for large-scale high-data volume experiments.

FIELD DEPLOYMENT AND EXPERIMENTS

An east-west line of stations was deployed with shot-point-to-station distances ranging from 90 to 2250 m (Table 1). Five stations were deployed west of the shot points and one was deployed northeast, outside of the quarry. Two shots were recorded by GEOS instruments, one on 11-22-85 and one on 11-26-85. The same stations used for shot #1 were used for shot #2, except for the station closest to the shot point (G1A-1 for shot #1 and G1A-2 for shot #2). Figure 1 is a map showing the quarry excavation, shot points and GEOS stations.

Stations G1A-1 and G1A-2 were deployed close to the shot points. They were equipped each with a three-component force-balanced accelerometer (Kinematics). Each channel was set to record at 400 samples/second. Stations G2G, G3G, and G4G were equipped with an accelerometer and a three-component velocity transducer (L-22, Mark Products) to assure high-quality unclipped recordings. Each channel recorded at 200 samples/second. Adjusting for attenuation, gains were increased with greater distance on both acceleration and velocity sensors. Station G5V was equipped only with a velocity transducer set to record at 400 samples/second. Station G6V was deployed on a grassy hill northeast of the quarry at the location of a permanent CALNET station. It was equipped only with a velocity transducer set to record at 400 samples/second.

Table 2 is a general description of site surroundings.

Instrument Programming and Performance

The six GEOS recorders were preset to record for several minutes at three possible shot times (11:30, 12:30 and 13:00 local time) to insure recording of the blast. The recorders were time-synchronized with a master clock (USGS #9) and clock errors were recorded as each data cartridge was removed. An amplifier and sensor calibration was also recorded before data cartridge removal.

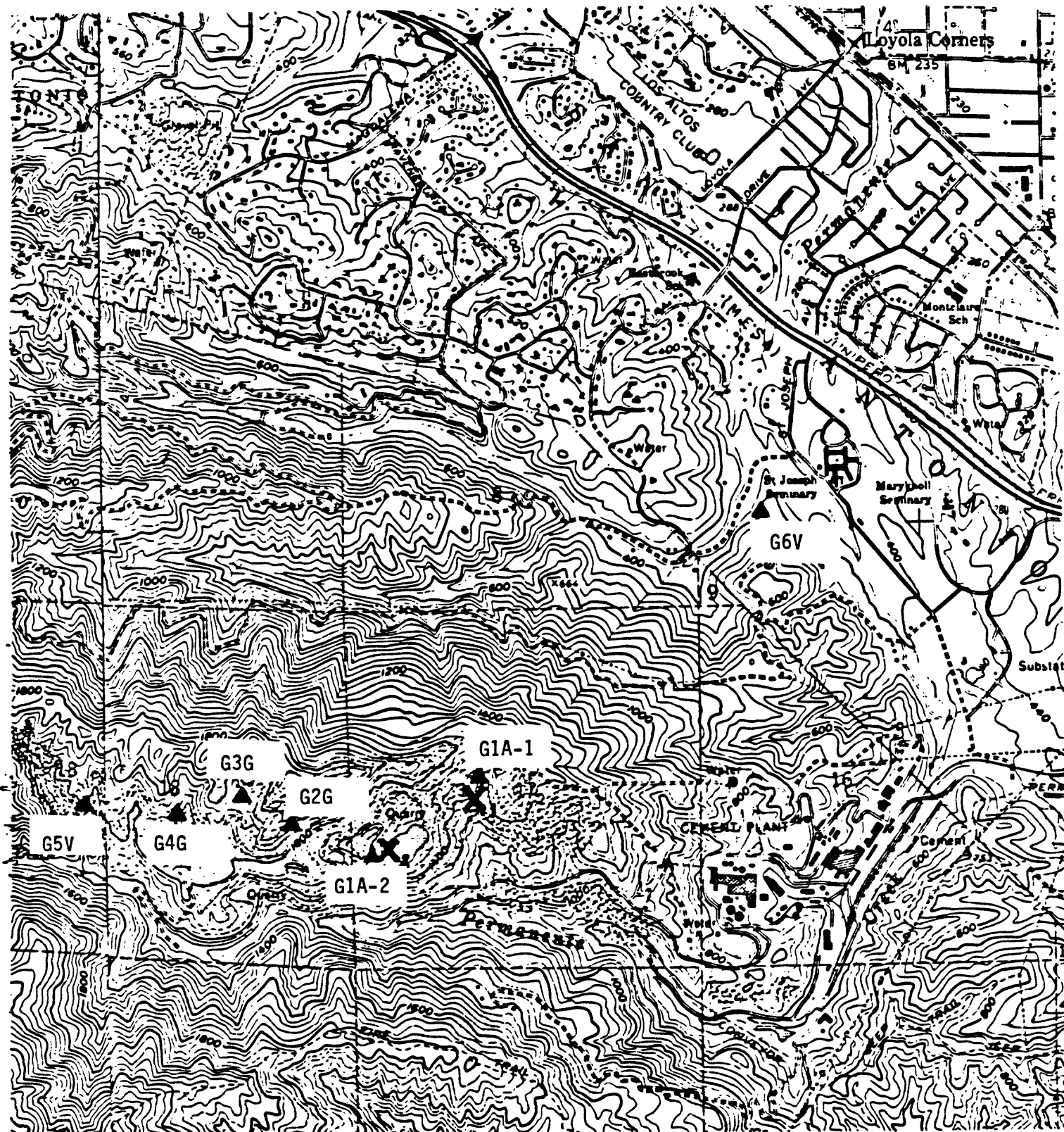


Figure 1

- ✕ Shot Points
- ▲ GEOS Stations



QUADRANGLE LOCATION
From U.S.G.S.
Cupertino, CA 7.5'
Quadrangle



CONTOUR INTERVAL 40 FEET

Shot #1 occurred at approximately 11:30:01 (local time) on 11/22/85 on the upper quarry wall consisting mostly of fill. It was considered a "clay shot" since mostly fill and little solid rock was blasted.

No data was recorded at stations G1A-1 and G4G for shot #1. Good acceleration or velocity records were obtained from stations G2G and G3G, and good velocity records were obtained from stations G5V and G6V. (Horizontal velocity channels clipped at station G3G.) A summary of peak amplitude counts and peak ground motion for shot #1 is shown in Table 3.

Changes in instrument recording parameters were made from an analysis of data from shot #1, and from the expectation of higher energy release from shot #2 due to coupling with the water table.

The instrument at station G1A-1 was removed from the site since it failed. A different GEOS recorder was deployed at the new station G1A-2. Gains were reduced from 12dB to 6 dB.

Gains on acceleration channels of station G2G were increased from 12 dB to 18 dB since the value of the maximum amplitude counts for shot #1 was only 110. Velocity channels remained at 36 dB. Gains on velocity channels at station G3G were decreased since horizontal channels clipped on shot #1. Gains on velocity channels at stations G5V and G6V were reduced since counts from shot #1 were high.

The instruments were again set for three pre-set recording times of 11:30, 12:30 and 13:00 (local time). The second shot occurred at approximately 11:31:00 (local time) and was recorded on all existing channels of all six stations. The blast shattered solid rock, and ground movement was noticeable at the top of the excavation.

Good records were obtained on all existing channels for shot #2. Table 4 is a summary of the peak amplitude counts and peak ground motions recorded at the six stations.

DESCRIPTION OF PLOTS

Table 5 is an explanation of the data plots shown in Figures 1-41. They include record sections, one-second enlarged acceleration plots, three-component seismograms, vertical-component Fourier amplitude spectra, and spectral ratios. The plots were obtained using

software developed by E. Cranswick.

Record sections (Figures 1-6) have been plotted showing closest to furthest stations (left to right) from the shot point. Peak amplitude counts are printed on the lower horizontal boundary below each seismogram. Three-character station codes followed by "A" (acceleration) or "V" (velocity) are printed on the upper horizontal boundary. Universal time (GMT) printed across the tops of the records corresponds to the first sample time (time = 0 on the time scale). All record sections are 8 seconds in duration. Normalized amplitude scale (Figs. 1-4) is defined by the arrow in the upper left of the page. The length of the arrow corresponds to the largest amplitude length of all of the seismograms. Record sections (Figs. 5-6) are plotted to an amplitude scale defined by the upper left arrow, a specific printed value in cm/s. One-second enlarged acceleration plots (Figs. 7-9) have a peak amplitude of $3 \times$ the upper left arrow length and are 1-second in duration.

The three-component seismograms are plotted to a unit peak amplitude length, the value of which appears in cm/s or cm/s² to the upper left of each seismogram. Component orientation and peak amplitude counts are displayed. Universal time (GMT) followed by the 3-character station code is printed at the top of the plots. (Seconds are letter-coded, and "A" for acceleration or "V" for velocity precedes the station code.) Acceleration plots are 8 seconds in duration.

The 'J' cosine-tapered spectral window is plotted on all vertical components of the three-component seismograms. All windows were centered on the initial *P*-break of each vertical seismogram. Baseline samples have been added (notable on some acceleration plots) in order to fit the 'J' spectral window. Spectra are plotted log-log scale with amplitude on vertical axis in cm/s and frequency on horizontal axis in Hz. Spectra exhibiting frequencies up to 200 Hz are displayed for stations with Nyquist frequencies of 200 Hz.

PRELIMINARY ANALYSIS

Preliminary analysis of spectra clearly show that seismic energy up to 100 Hz was well recorded above background noise. Multiple *P*-arrivals are evident from the sequential

ripple blasting of each shot.

Record sections showing relative amplitudes for shot #1 and shot #2 (Figures 5 and 6) exhibit different ground motion characteristics at the defined stations for each shot. Shot #1 was blasted in an upper quarry wall of mostly fill, while shot #2 was blasted in the quarry bottom in hard rock and close to the water table. Comparison of spectra for shots #1 and #2 indicate that shot #2 produced generally higher frequencies and larger amplitudes than shot #1. A prominent peak in the 25–30 Hz range is very notable in spectra of both shots, but it is less notable in shot #2 spectra since shot #2 produced similar amplitudes both below and above the 25–30 Hz range. Comparison of Tables 3 and 4 show that peak ground motions were larger for shot #2 than for shot #1 except at the two outer stations (G5V and G6V). Notable from Table 3 is the larger peak velocity (.038 cm/s) at station #6 (1850 m from shot #1) than the peak velocity (.023 cm/s) at station 2 (771 m from shot #1).

ACKNOWLEDGMENT

The data set in this report was obtained from software developed by E. Cranswick and G. Maxwell.

REFERENCE

Borcherdt, R. D., Fletcher, J. B., Jensen, E. G., Maxwell, G. L., Van Schaack, J. R., Warrick, R. E., Cranswick, E., Johnston, J. J. S., and McClearn, R., A general earthquake observation system: *Bull. Seismol. Soc. Am.* 75, no. 6.

TABLE 1

Station	Distance From Shot #1 (Elev. = 1400') (meters)	Distance From Shot #2 (Elev. = 1140') (meters)	Station Elevation (meters)
G1A-1	128	...	402
G1A-2	...	90	360
G2G	771	407	463
G3G	1066	728	549
G4G	1339	984	541
G5V	1784	1370	530
G6V	1850	2250	122

TABLE 2

Station	Site Surroundings
G1A-1	Upper quarry wall consisting of mostly fill material. Soil is gravel and clay.
G1A-2	Bottom of quarry excavation. Hard rock. Sensor in gravelly sand.
G2G	Upper rim of quarry excavation. Hard Rock. Sensor in gravelly sand.
G3G-G5V	Gravel roads above main excavation. Hard rock and gravelly sand.
G6V	Grassy hill near CALNET station outside of quarry. Sensor 10' south of VCO tub in clay soil.

TABLE 3
(Shot #1)

Station	Peak Amplitude Counts	Peak Ground Motion
G1A-1	no data	
G2G	Acceleration: 110 (N-S) Velocity: 2414 (N-S)	1.65 cm/s ² .023 cm/s
G3G	Acceleration: 258 (V) Velocity: 32767 (H clipped)	1.94 cm/s ² .040 cm/s
G4G	no data	
G5V	Velocity: 25647 (E-W)	.031 cm/s
G6V	Velocity: 31302 (V)	.038 cm/s

TABLE 4
(Shot #2)

Station	Peak Amplitude Counts	Peak Ground Motion
G1A-2	Acceleration: 11618 (V)	348 cm/s ²
G2G	Acceleration: 1980 (E-W) Velocity: 10374	14.9 cm/s ² .100 cm/s
G3G	Acceleration: 843 (V) Velocity: 25033 (E-W)	6.35 cm/s ² .121 cm/s
G4G	Acceleration: 734 (E-W) Velocity: 9949 (E-W)	2.78 cm/s ² .024 cm/s
G5V	Velocity: 10580 (E-W)	.026 cm/s
G6V	Velocity: 2857 (E-W)	.007 cm/s

TABLE 5
Explanation of Data Set

Figure(s)	Explanation
1 & 2	Record sections, all channels, shot #1 & #2, respectively.
3 & 4	Record sections, vertical channels, shot #1 & #2, respectively.
5 & 6	Record sections, vertical velocity channels, showing relative amplitudes.
7-9	One-second enlarged plots of shot #2, station 1 acceleration: channels 1: vert., 2: N-S, 3: E-W, respectively.
10-21	Shot #1: Station time histories, followed by vertical spectra (records of 5-second length are acceleration, 8-second are velocity). Note: Baseline samples have been added (notable on some accel.) plots in order to fit the "J" cosine taper spectral window.
22-39	Shot #2: Three-component seismograms followed by vertical-component spectra.
40	Spectral ratio: shot #1, station 2 vertical velocity divided by station 6 vertical velocity.
41	Spectral ratio: shot #2, station 2 vertical velocity divided by station 6 vertical velocity.

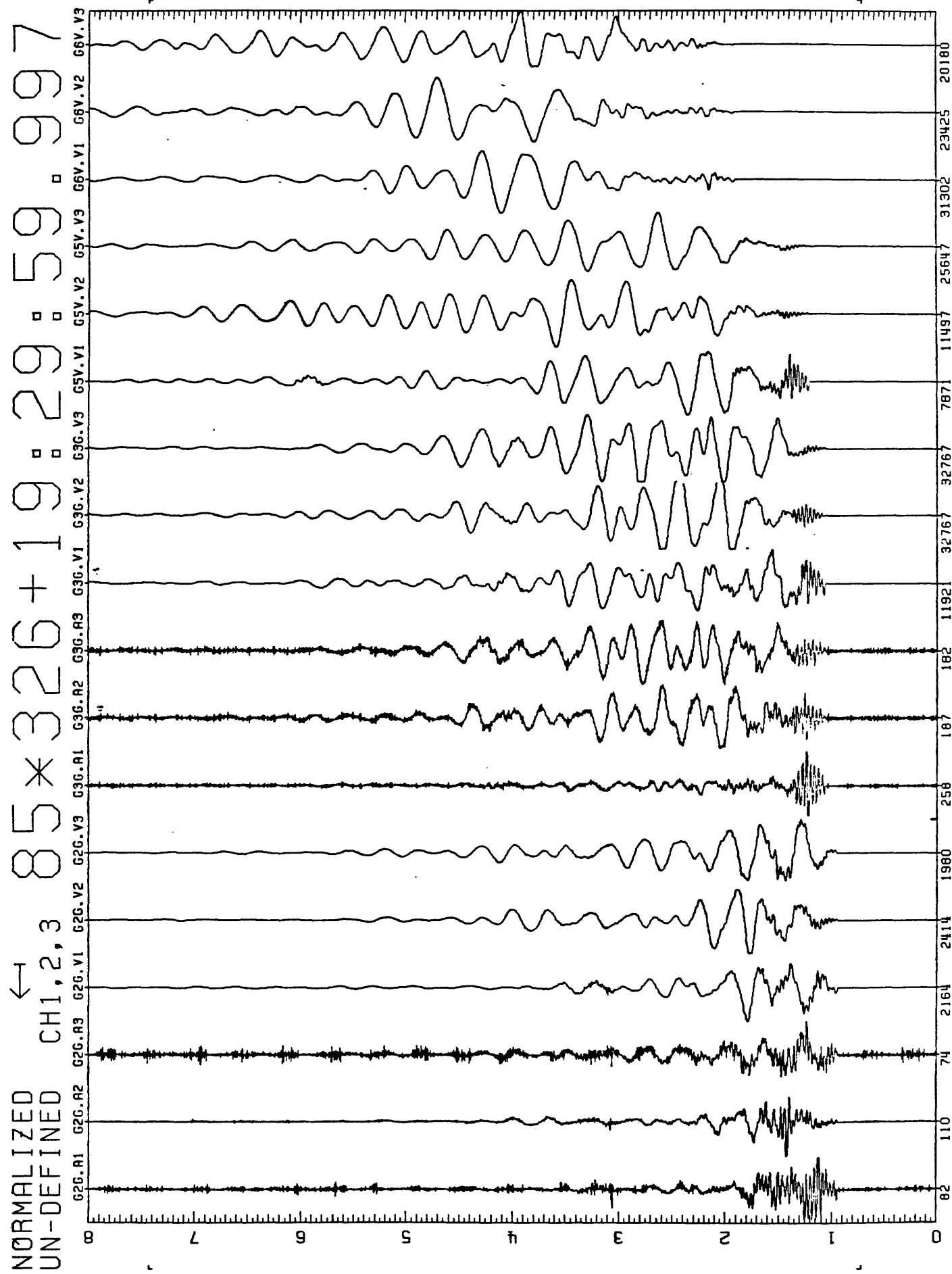


Figure 1

NORMALIZED
UN-DEFINED
CH1,2,3
85*330+19:30:59.997

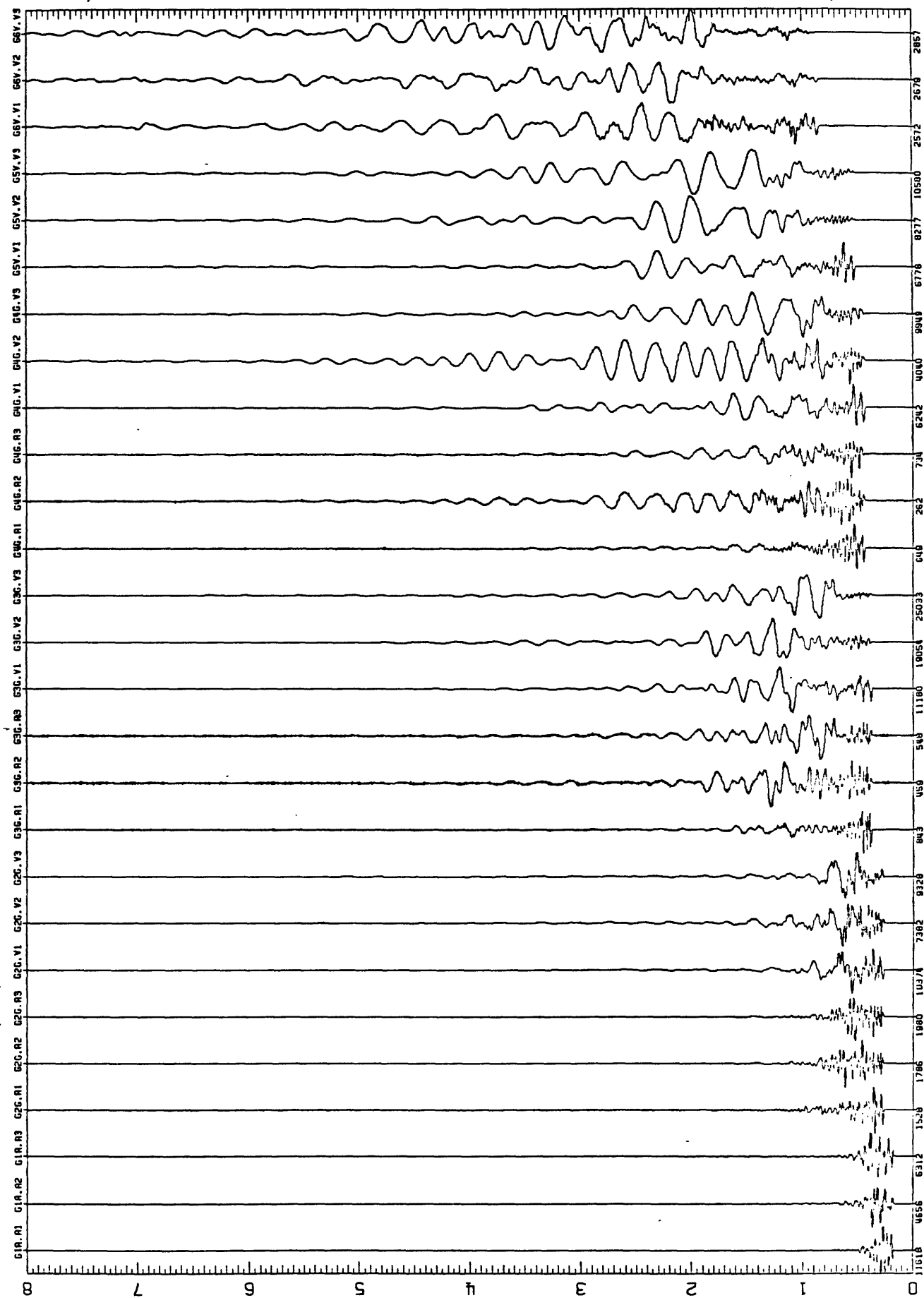


Figure 2

NORMALIZED
UN-DEFINED. CH1/UDF 85*326+19:29:59.997

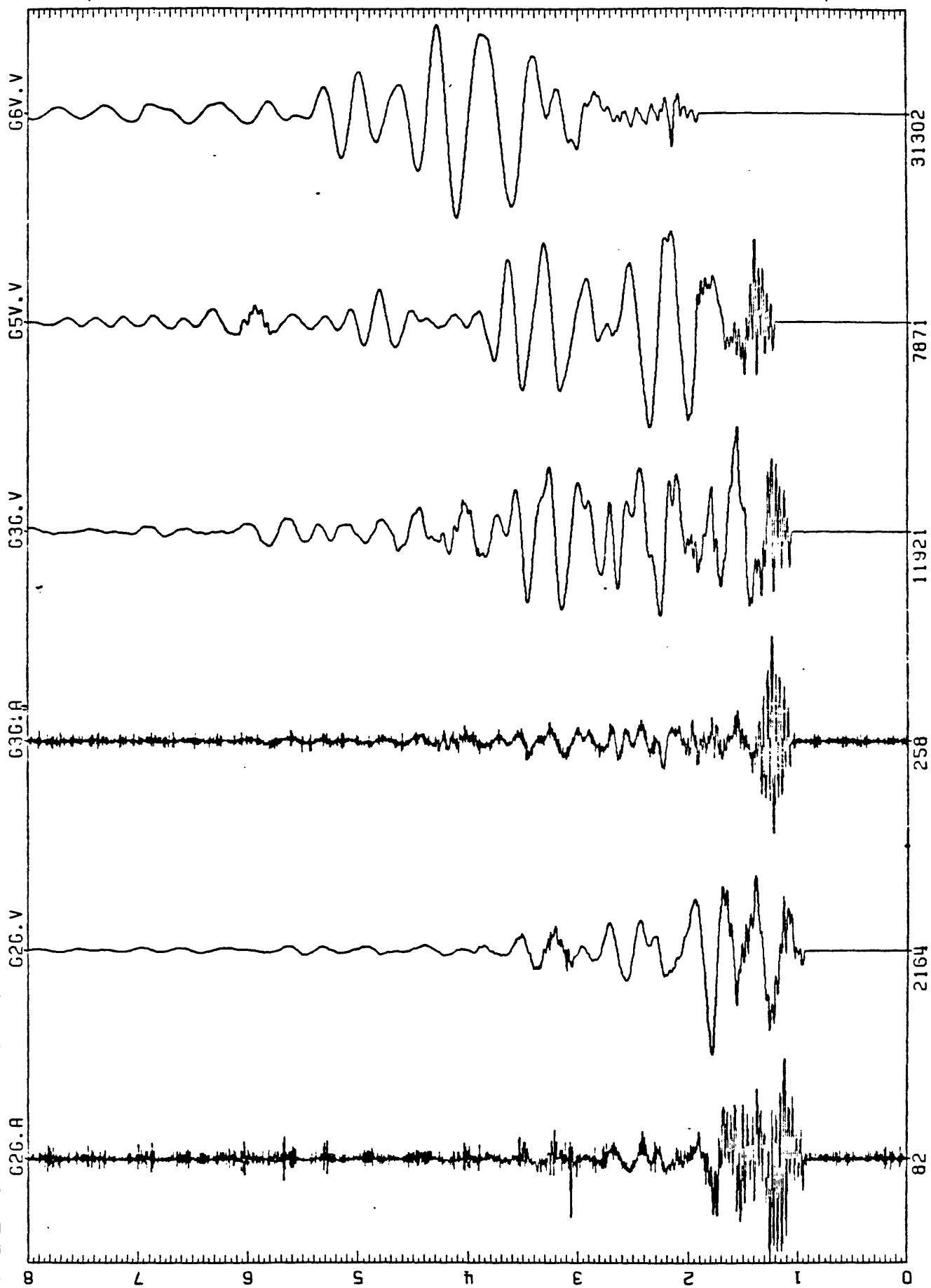


Figure 3

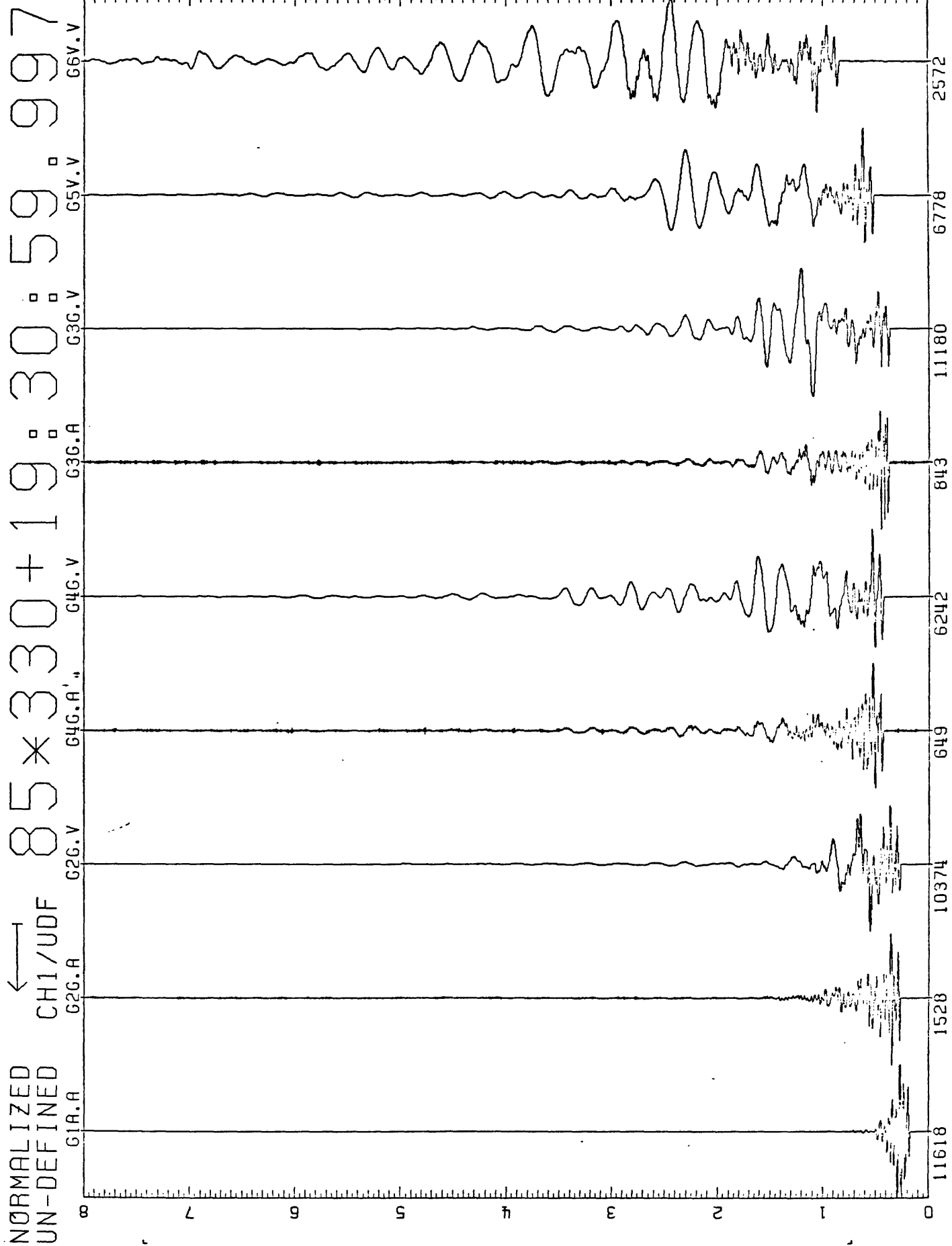


Figure 4

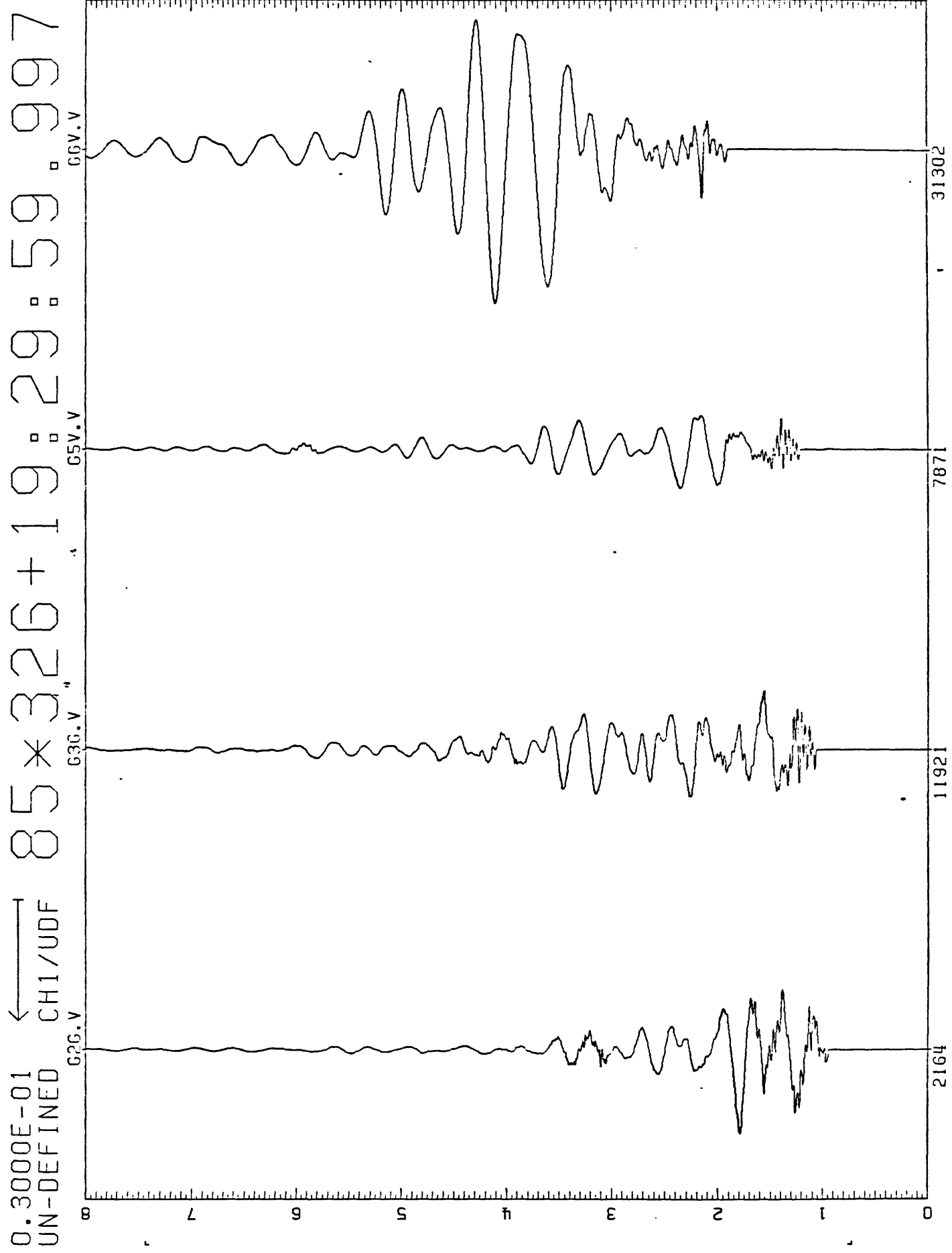


Figure 5

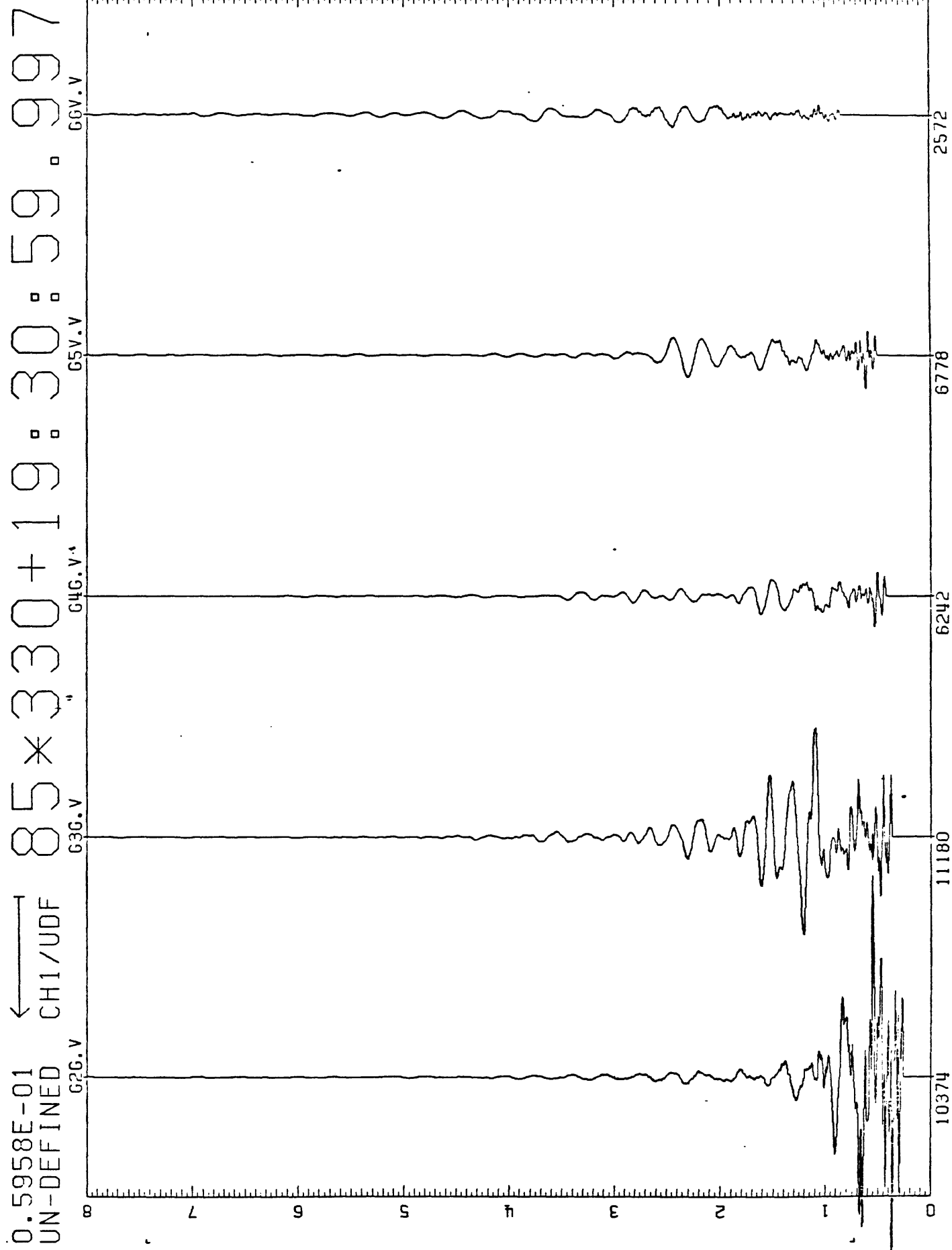


Figure 6

NORMALIZED
UN-DEFINED

← CH1/UDF

85*330+19:30:59.999

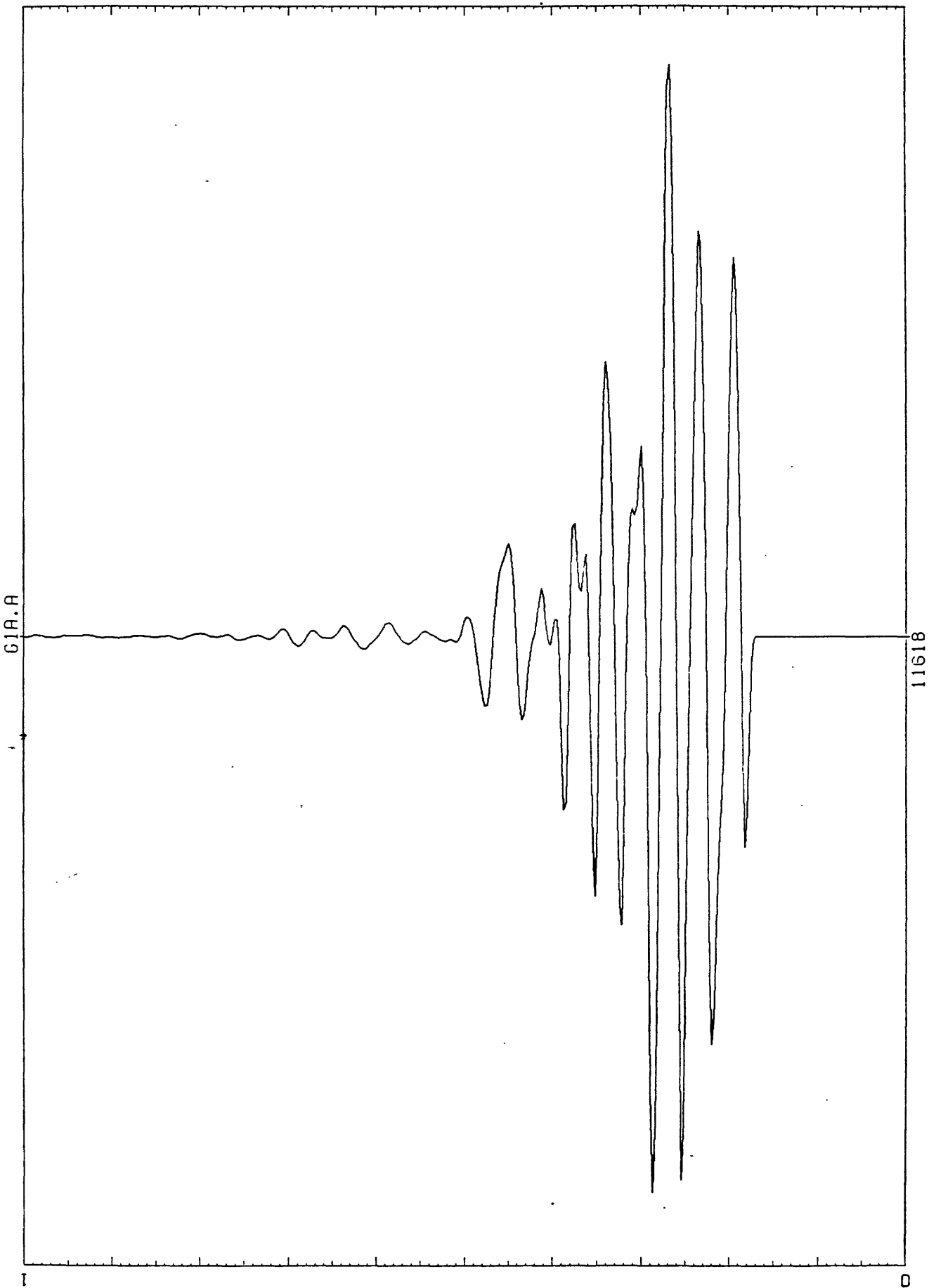


Figure 7

NORMALIZED ← 090/CH2 85*330+19:30:59.999
UN-DEFINED.

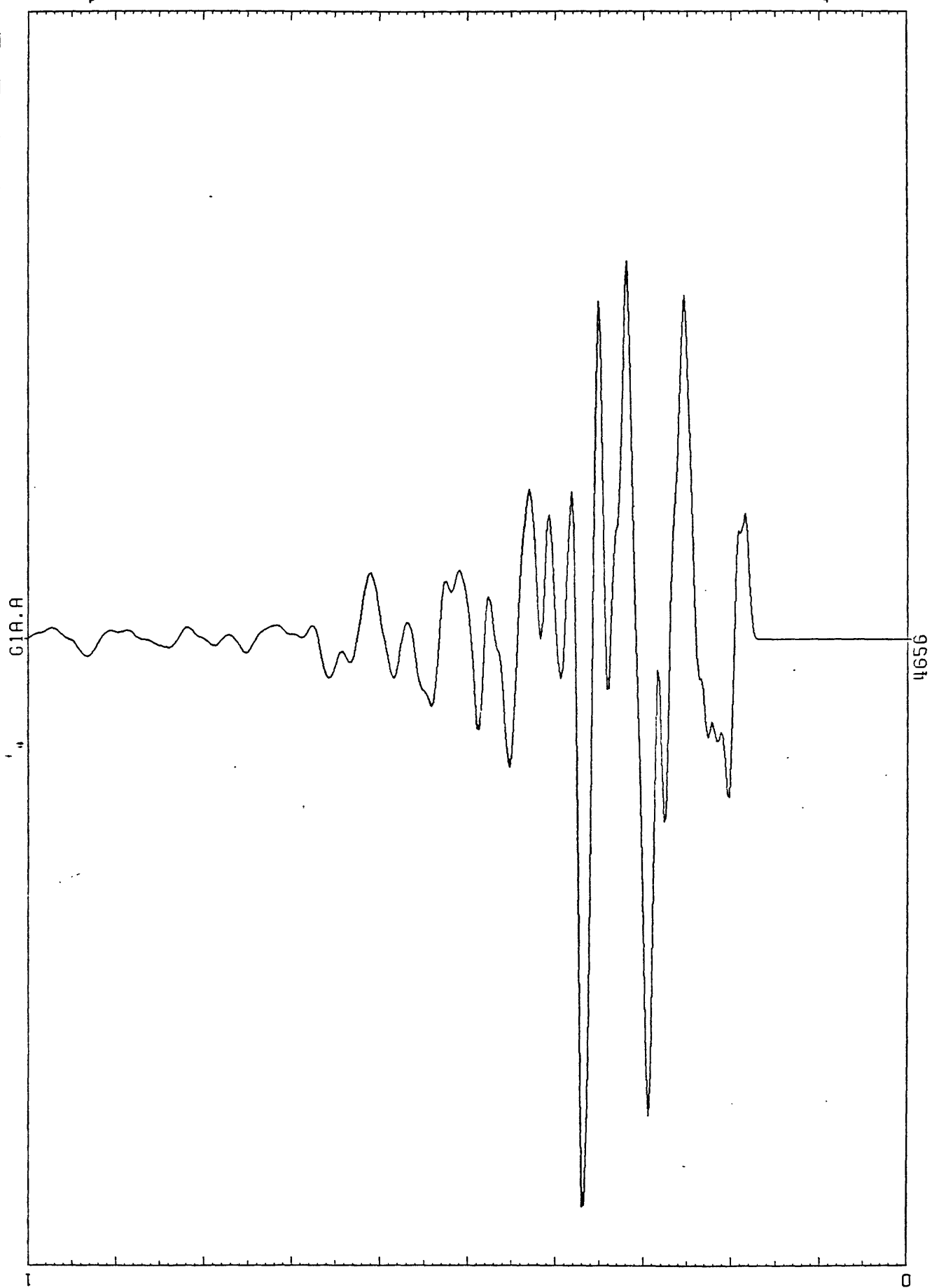


Figure 8

NORMALIZED ← 85*330+19:30:59.999
UN-DEFINED 090/CH3

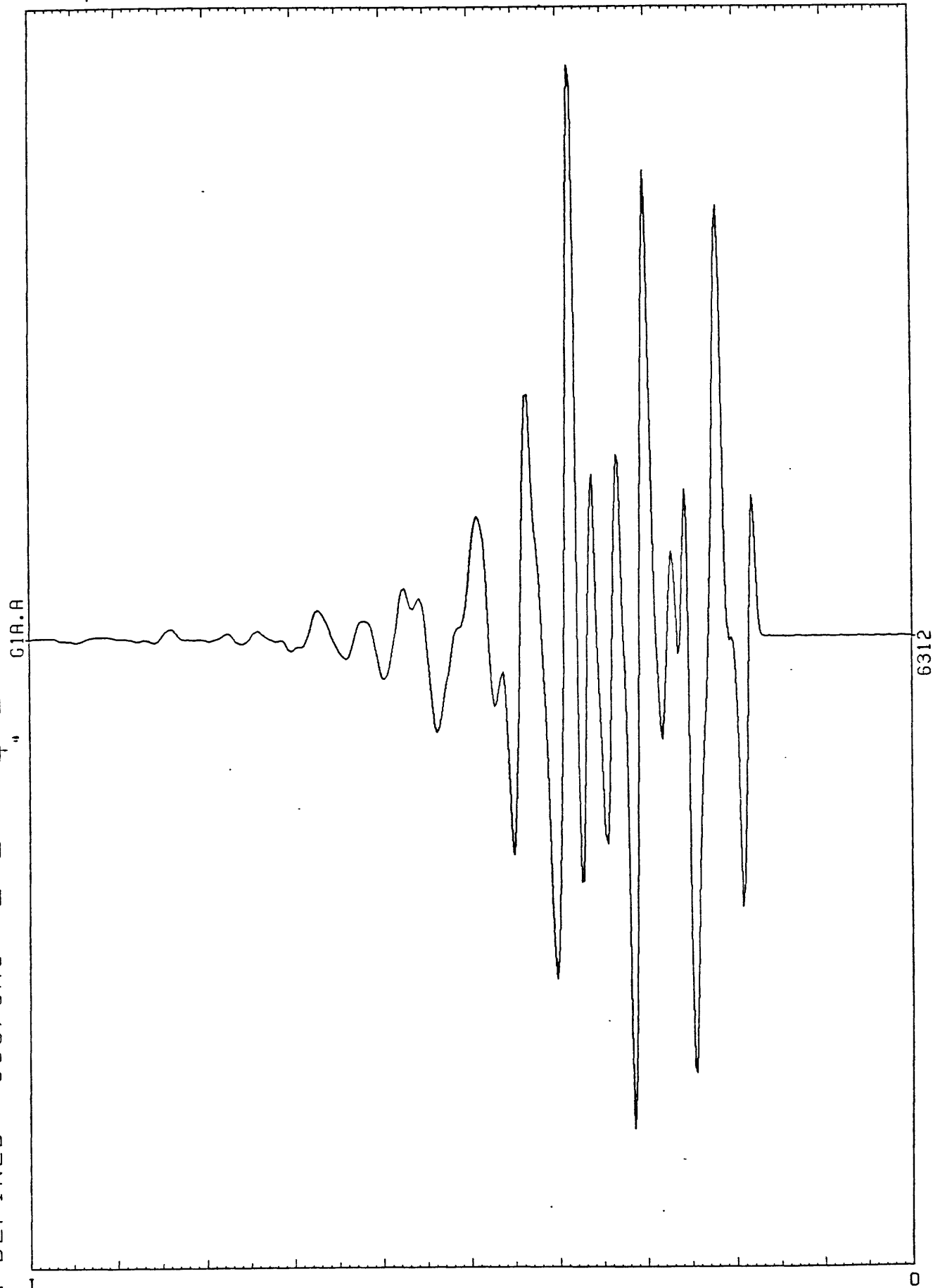


Figure 9

3261929TA.G2G

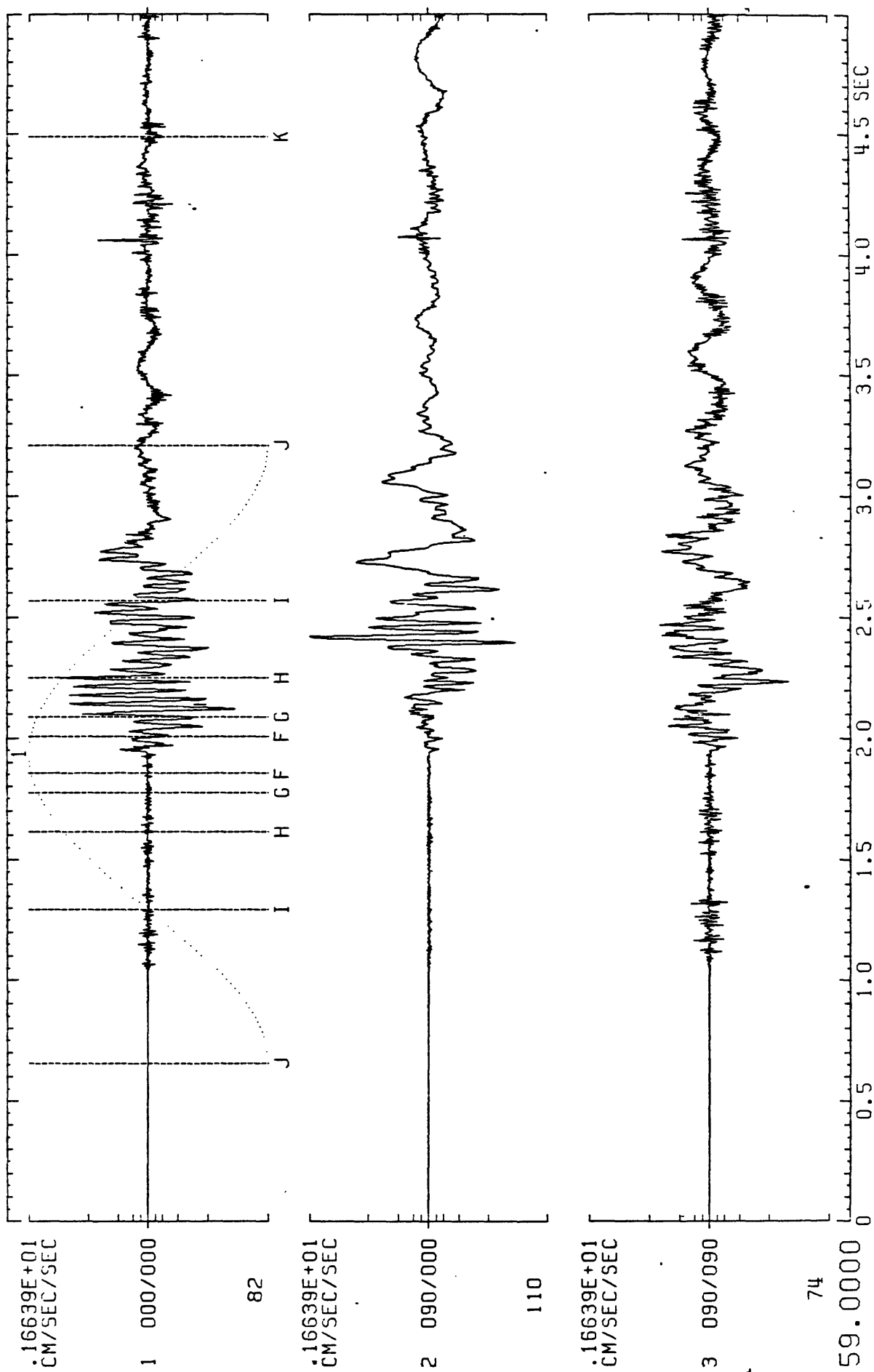


Figure 10

W#1=(C1 000/00007,00000188,J"),BL=0,CB=1,HP=1,ED=A"

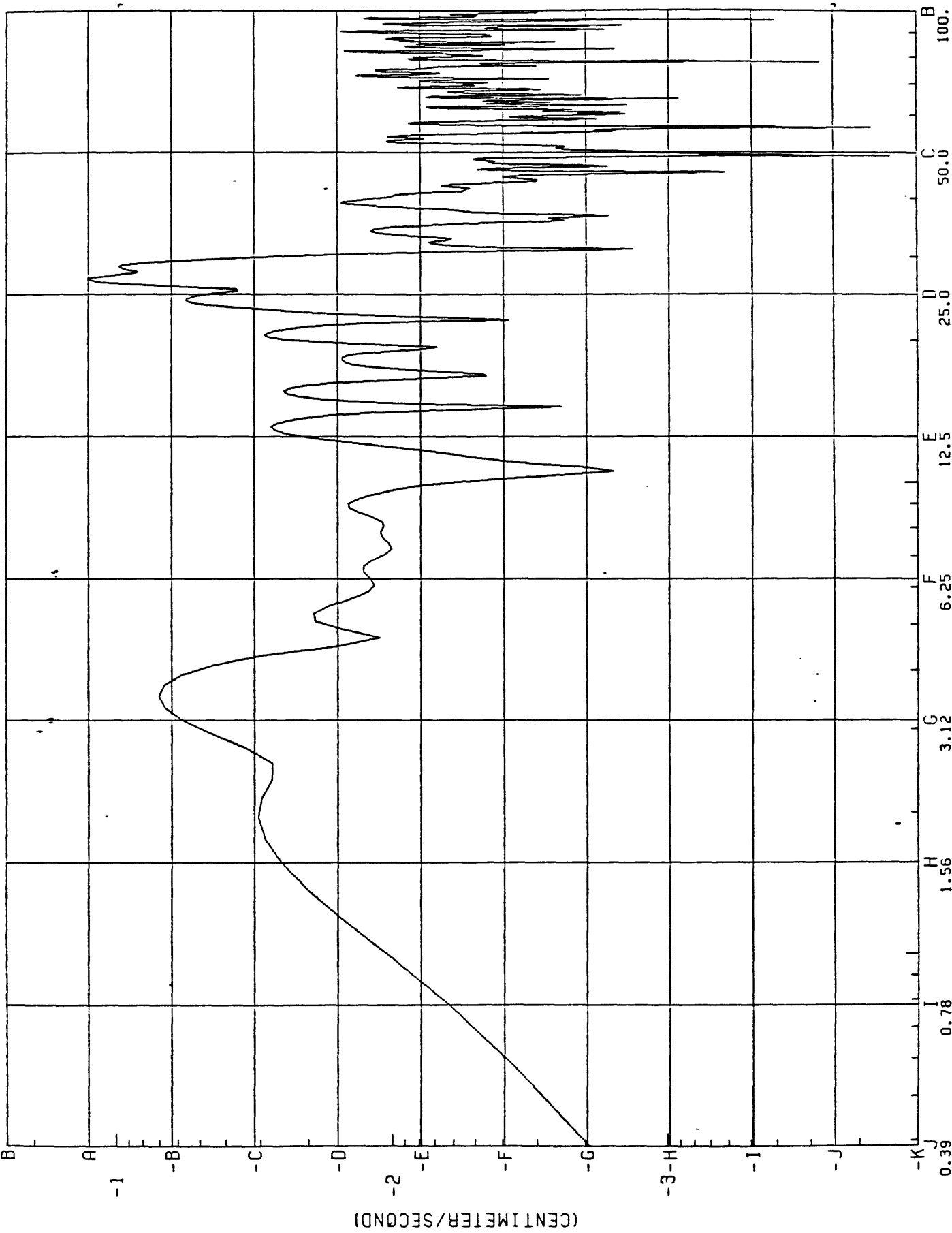


Figure 11

3261929TV.G2G

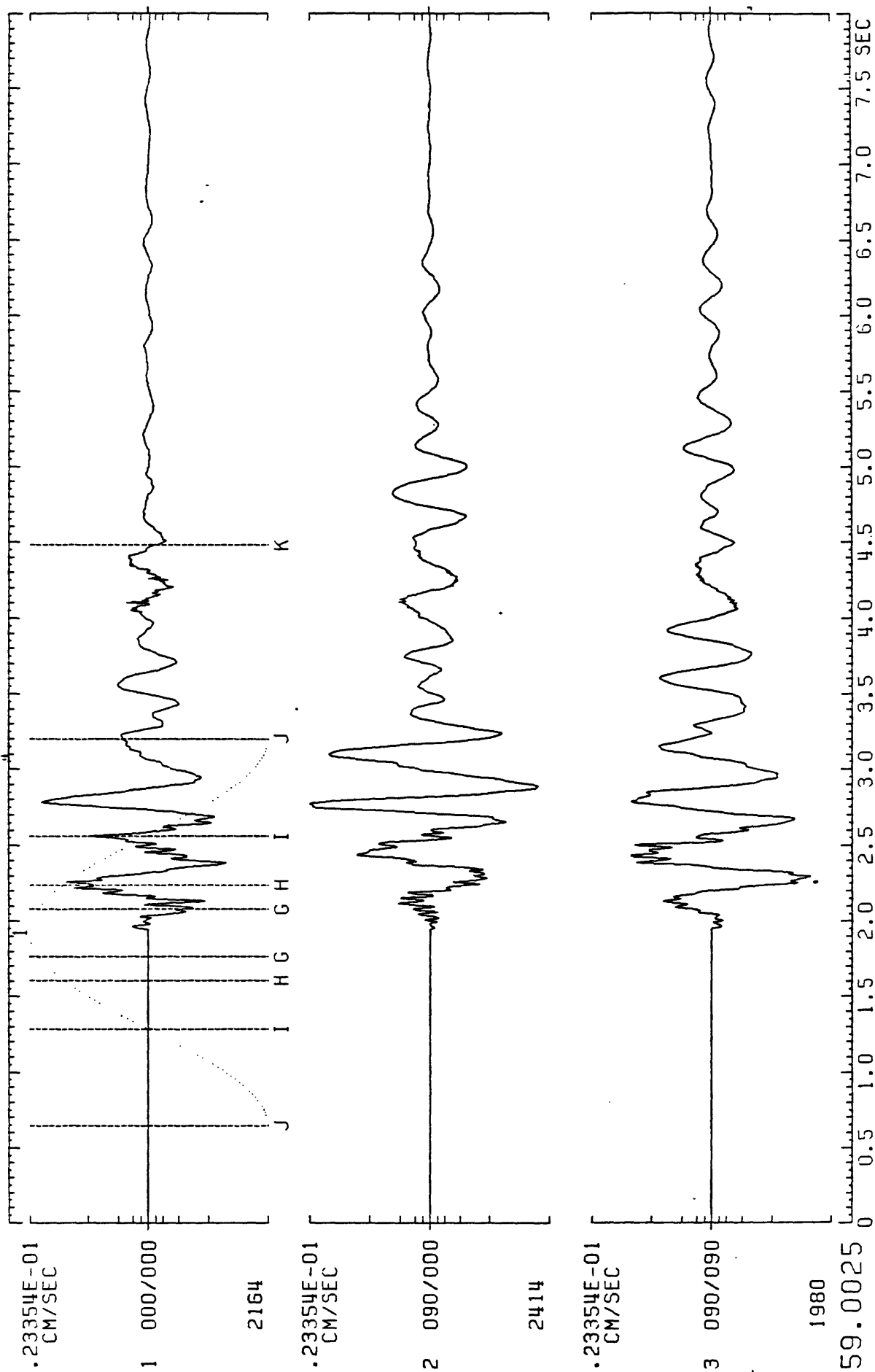


Figure 12

M*1=(C1 000/000J,0000186,J"),BL=0,CB=1,HP=1,ED=A"

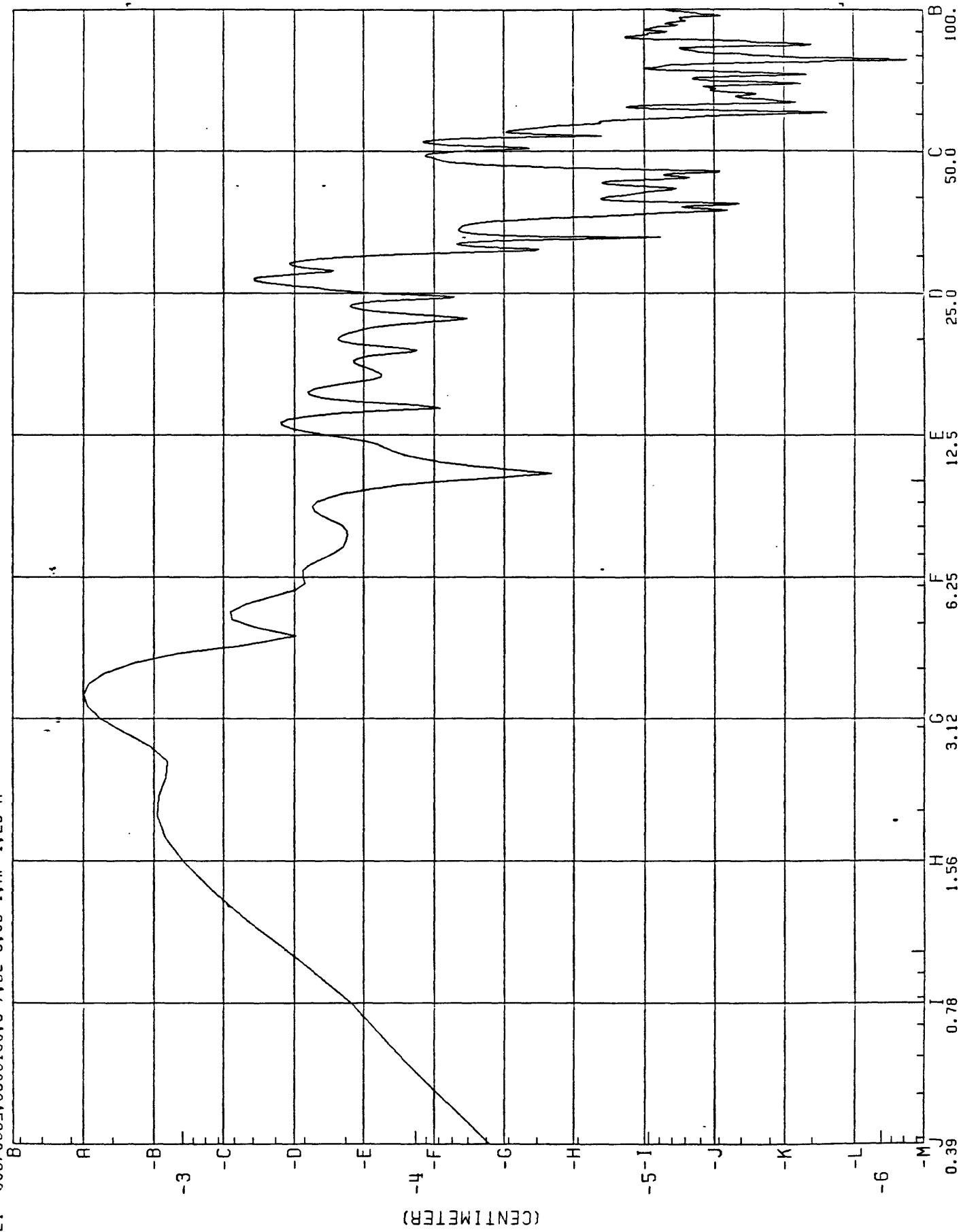


Figure 13

3261929TA.G3G

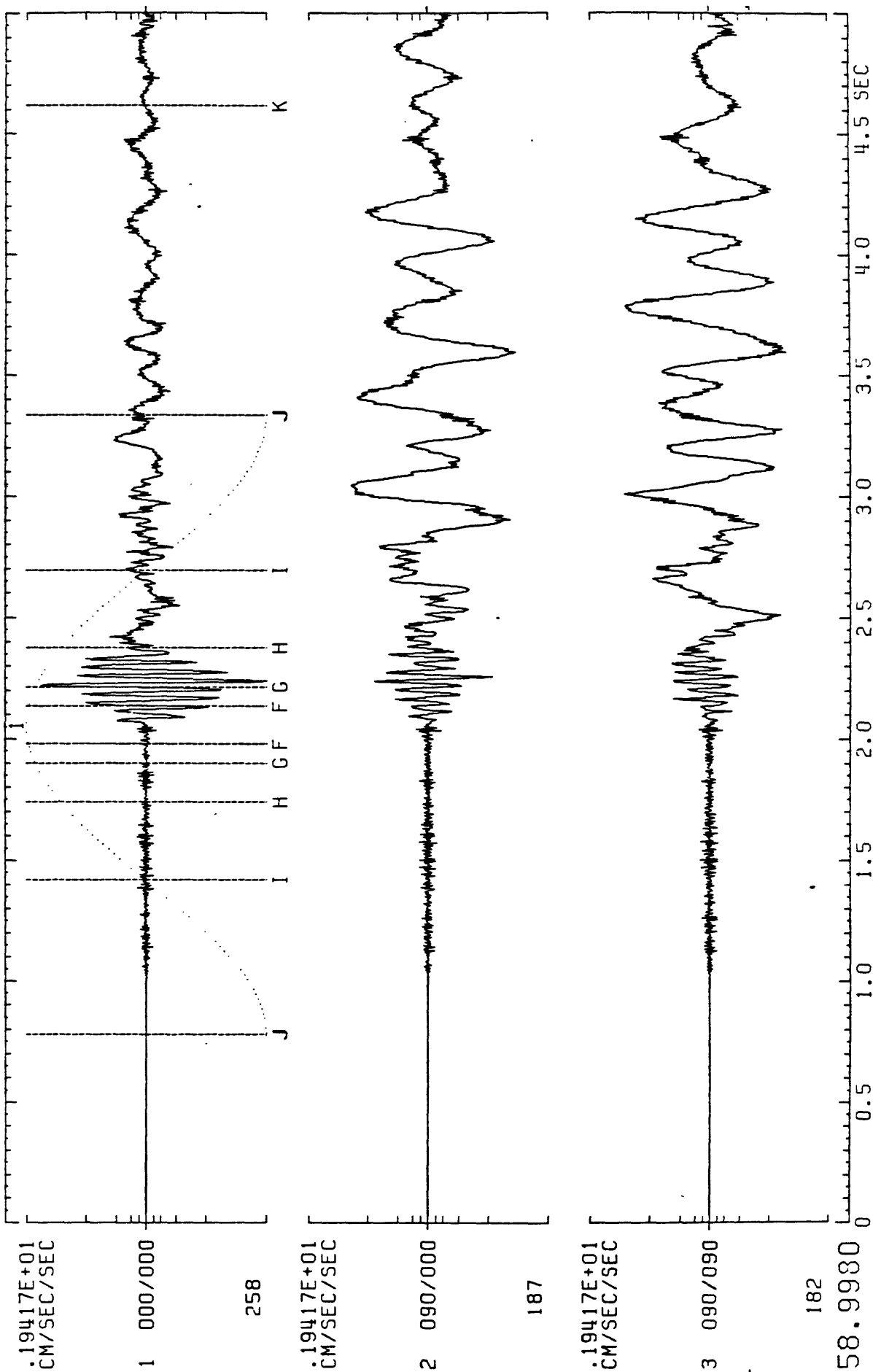


Figure 14

MOTION=ACCEL RAT S/S=200. SAM=01024 3261929TA.G3G

B=20 T=-20 L=+200

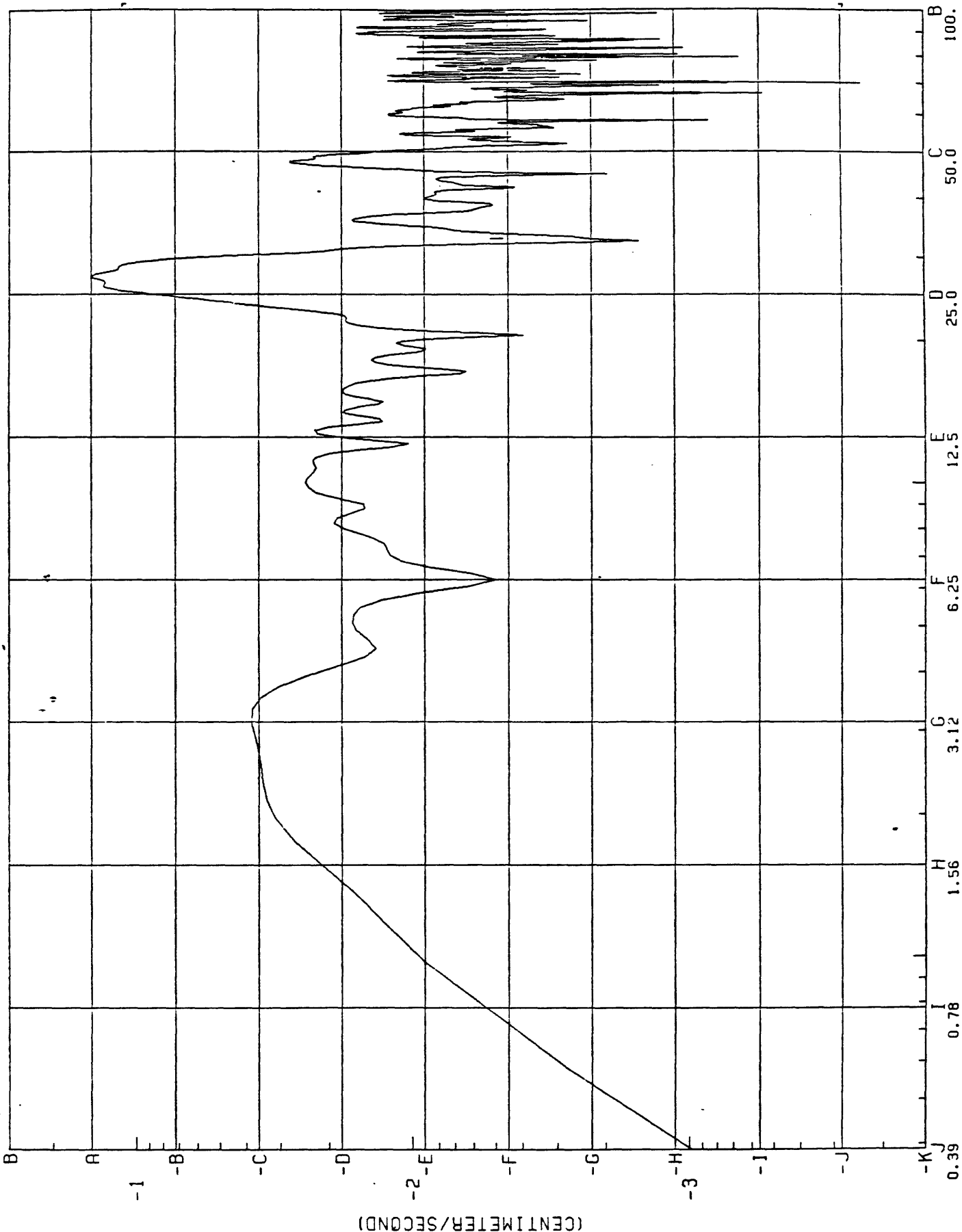


Figure 15

3261929TV.G3G

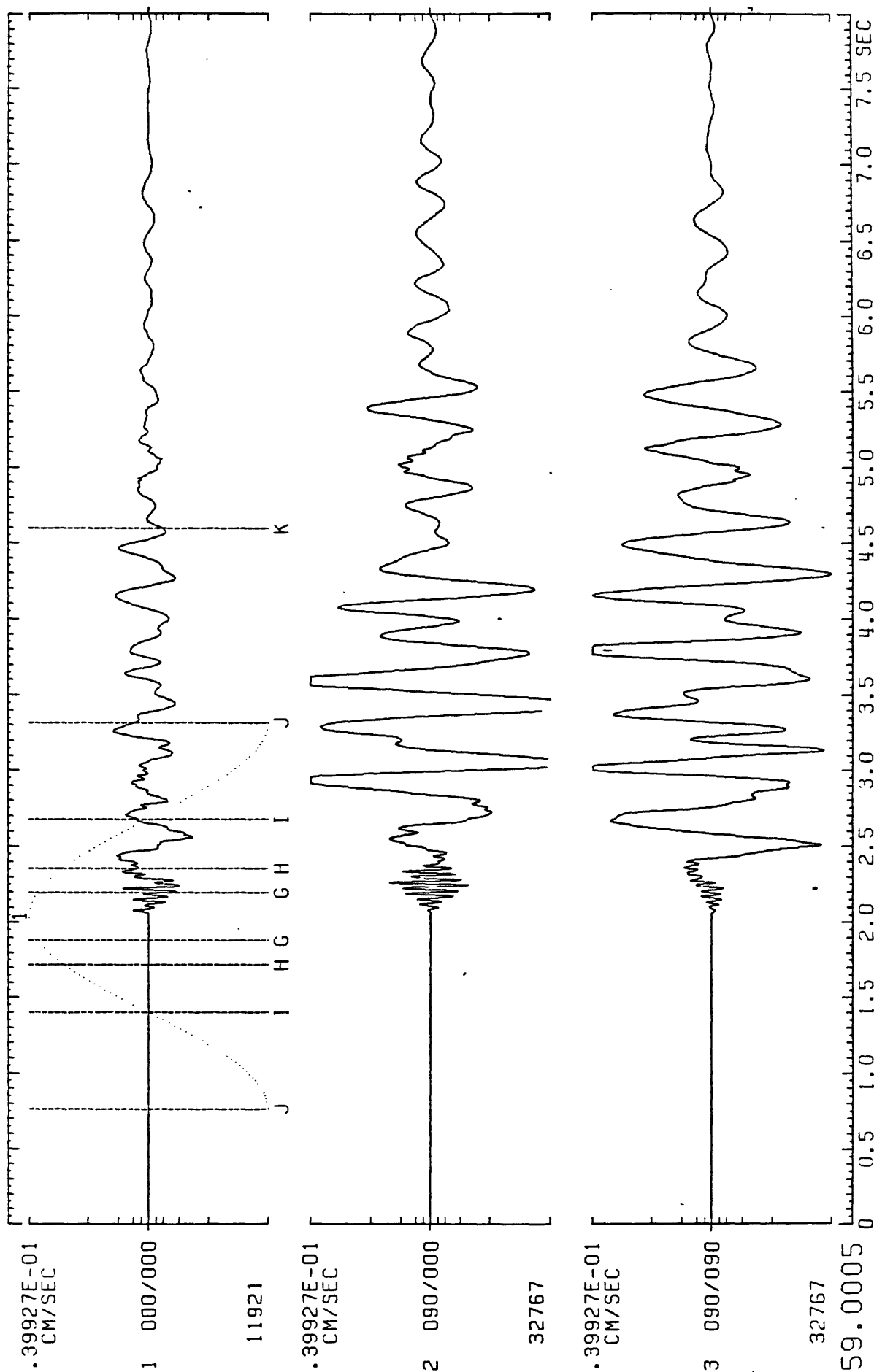


Figure 16

M*1=(C1 000/0003,0000209,J*),BL=0,CB=1,HP=1,ED=A*

MOTION=VELOCITY S/S=200. SAM=01024 3261929TV.G3G

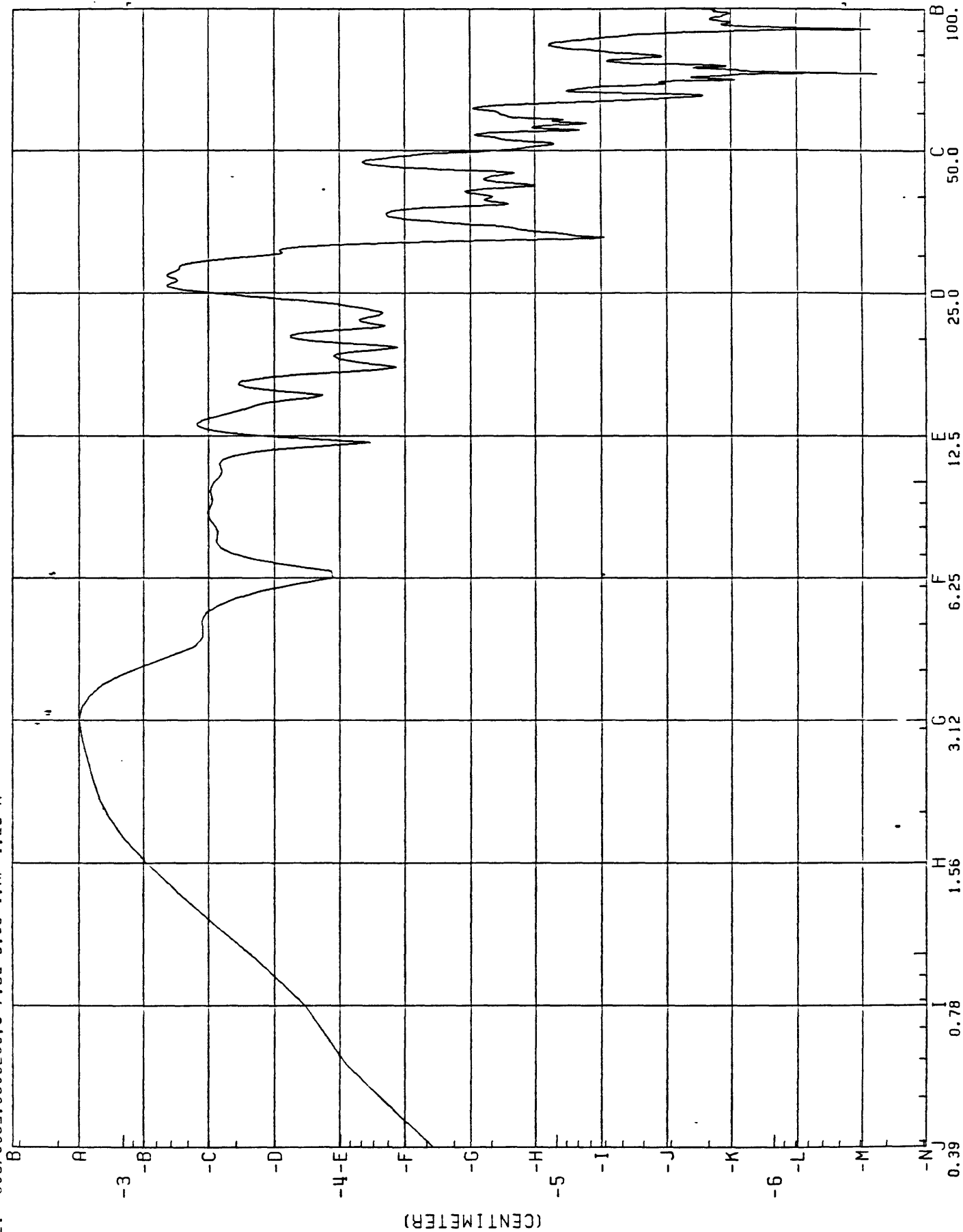


Figure 17

3261930AV.G5V

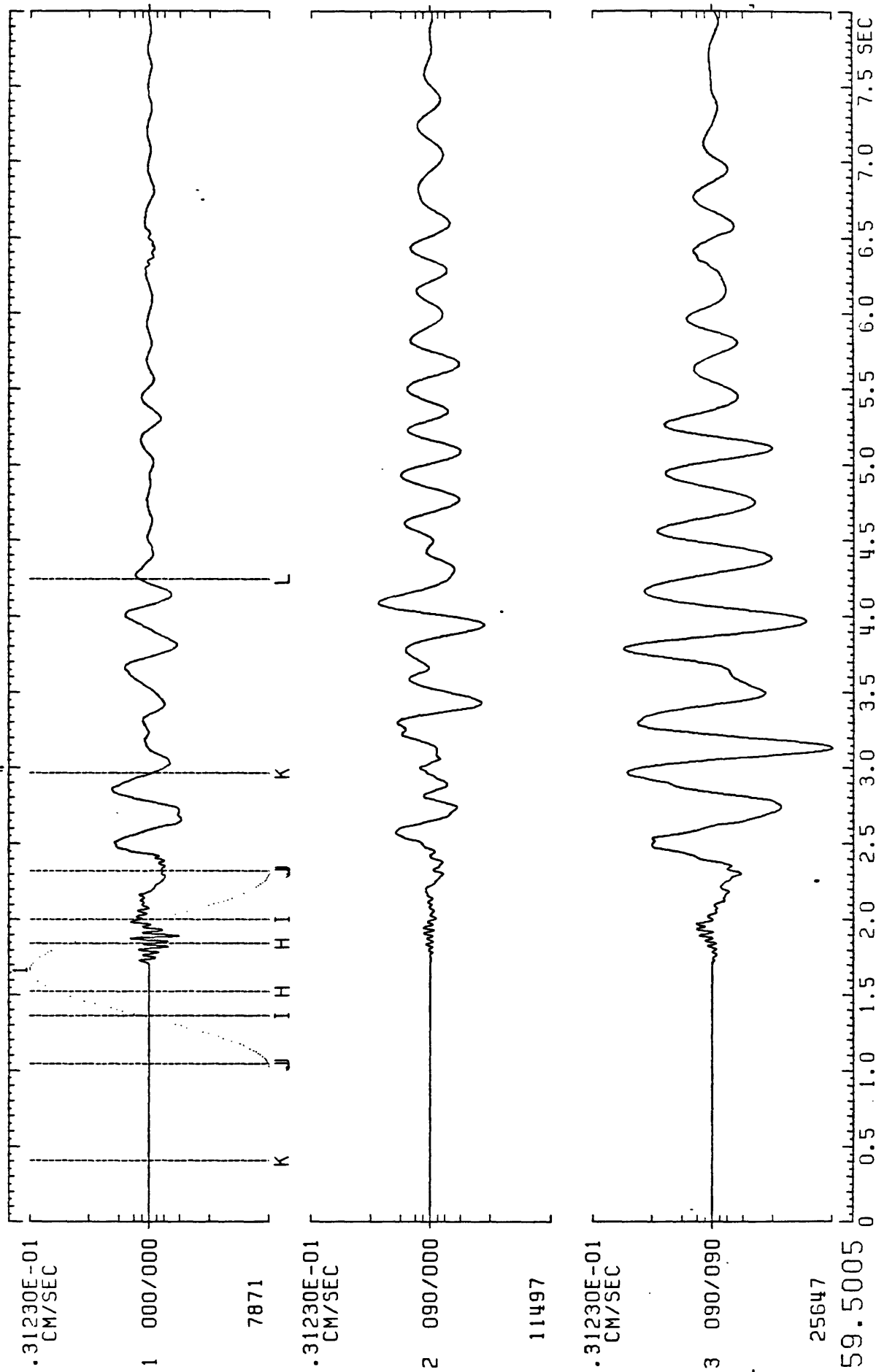


Figure 18

W*1=(C1 000/0000,00000468,J*),BL=0,CB=1,HP=1,ED=R*

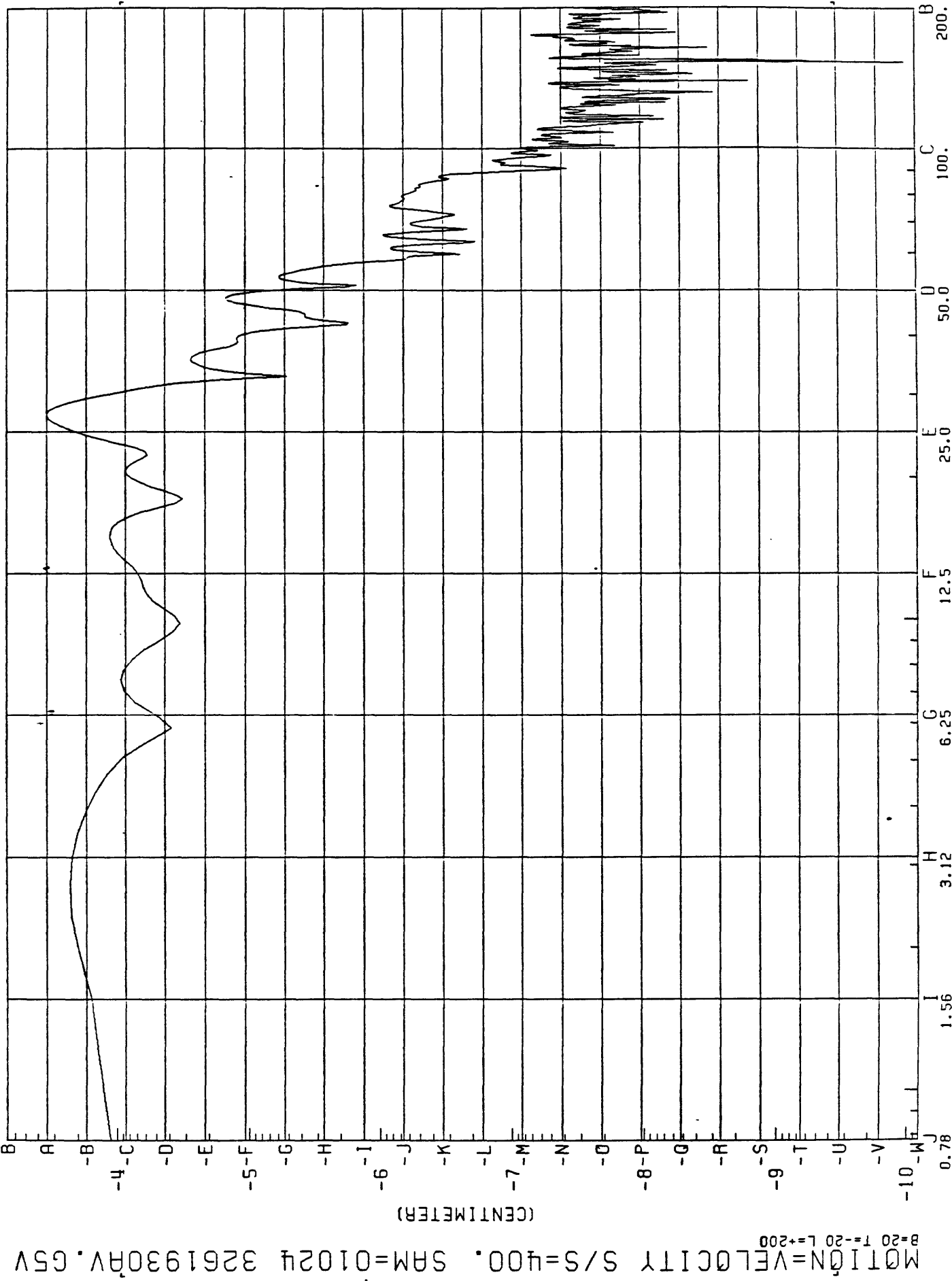


Figure 19

3261929TV.G6V

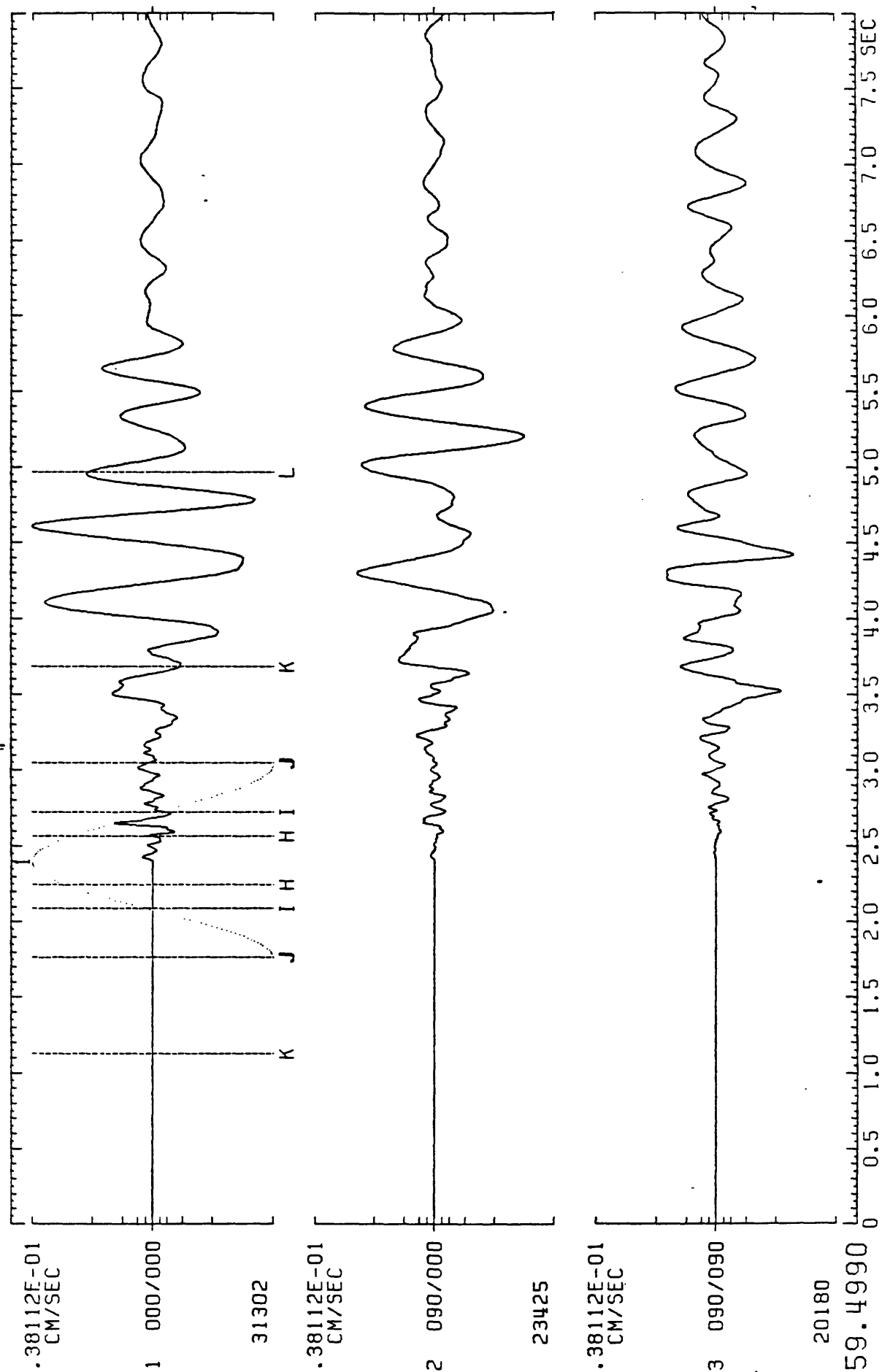


Figure 20

M#1=(C1 000/00007,0000760,J"),BL=0,CB=1,HP=1,ED=R"

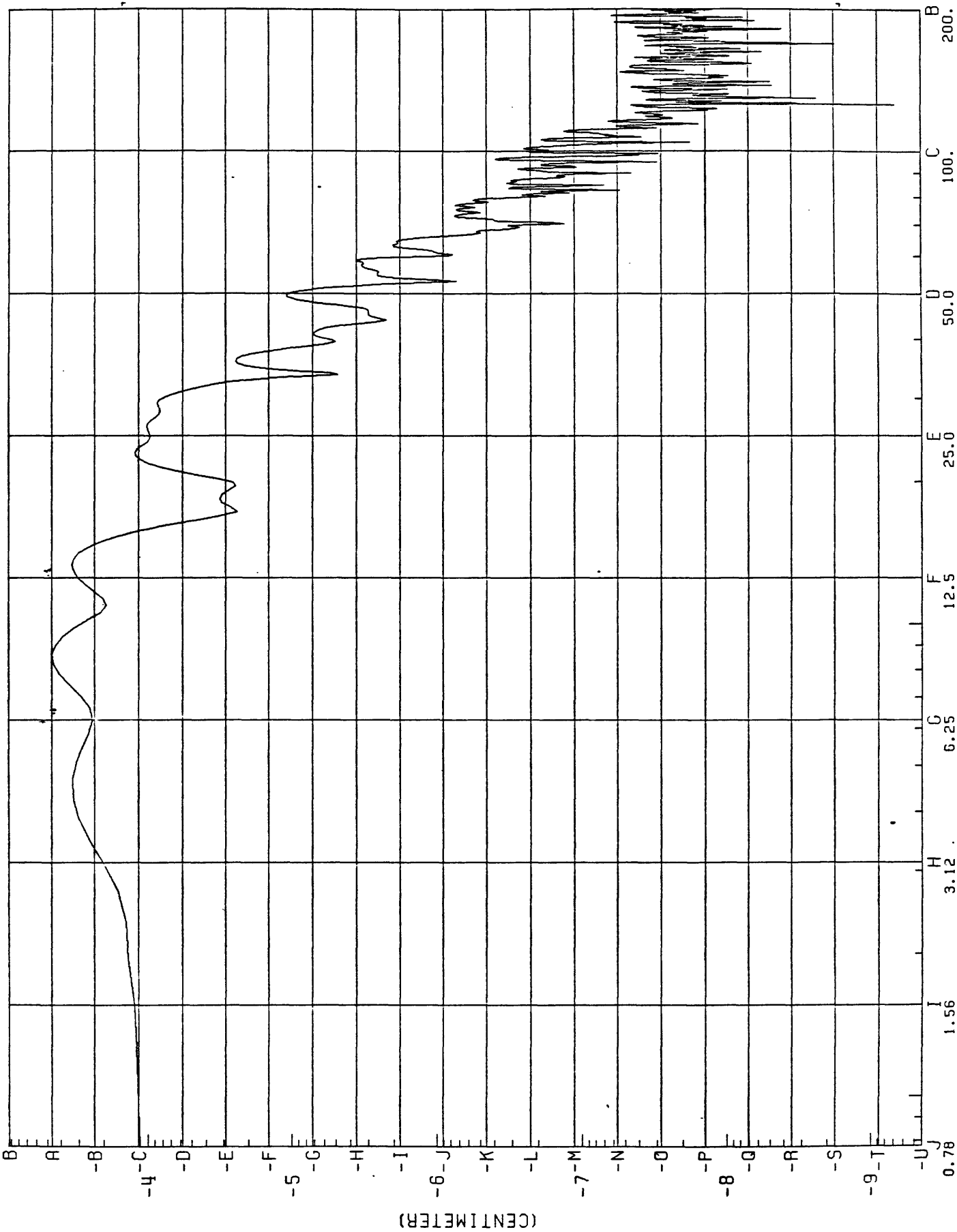


Figure 21

3301930TA.G1A

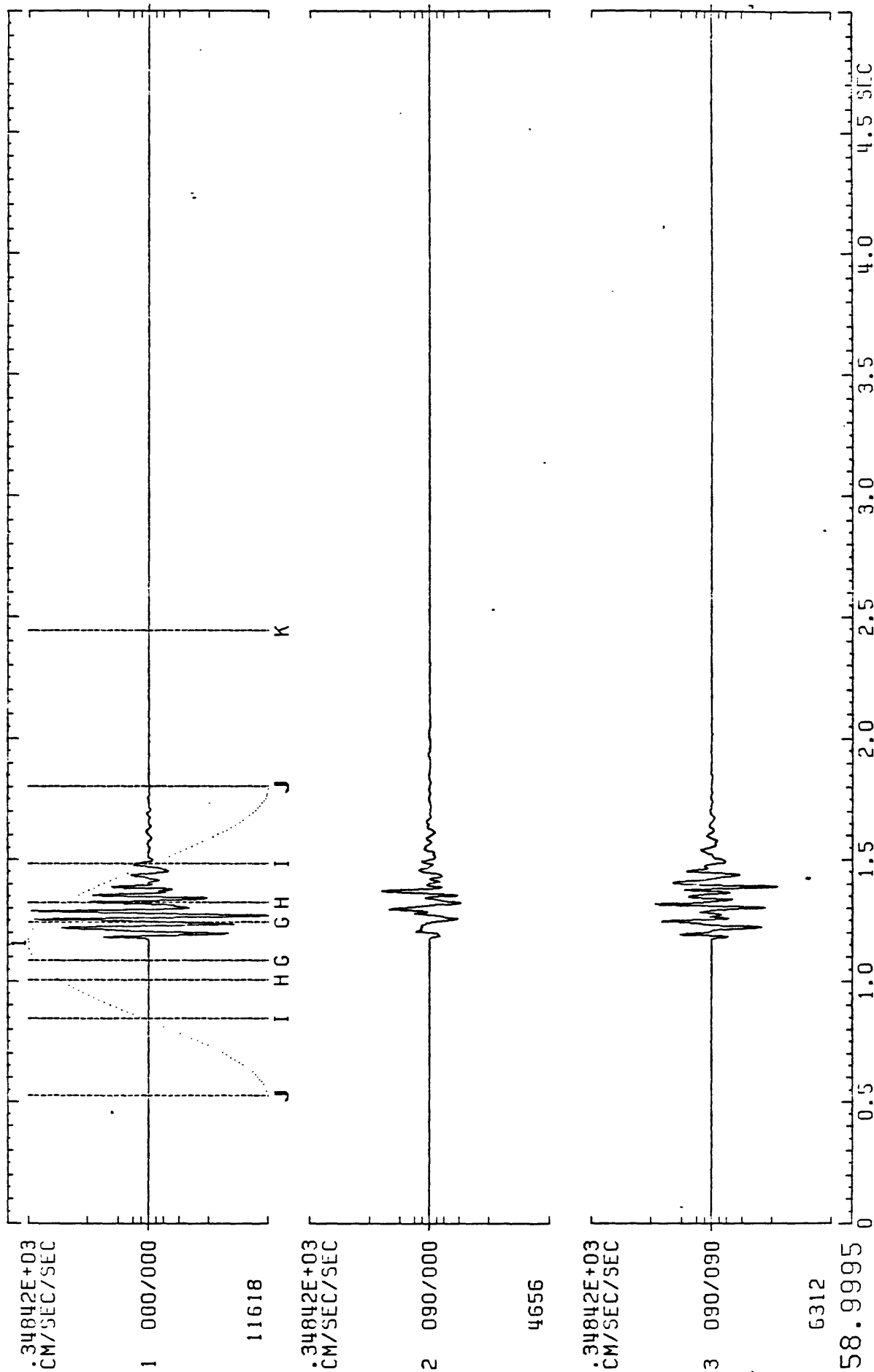


Figure 22

M#1=(C1 000/0000,0000064,J") ,BL=0,CB=1,HP=1,EO=A"

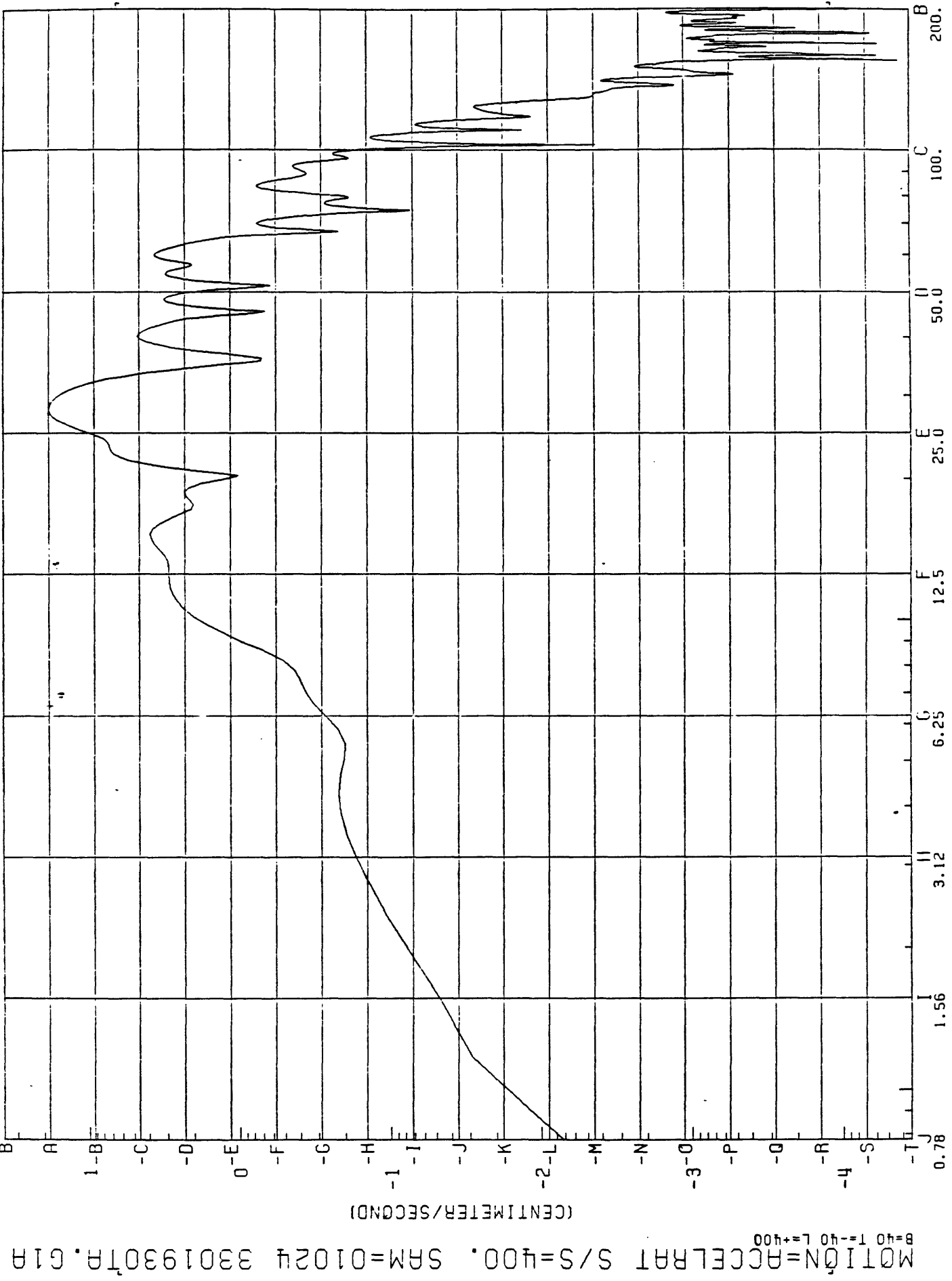


Figure 23

3301930TA.G2G

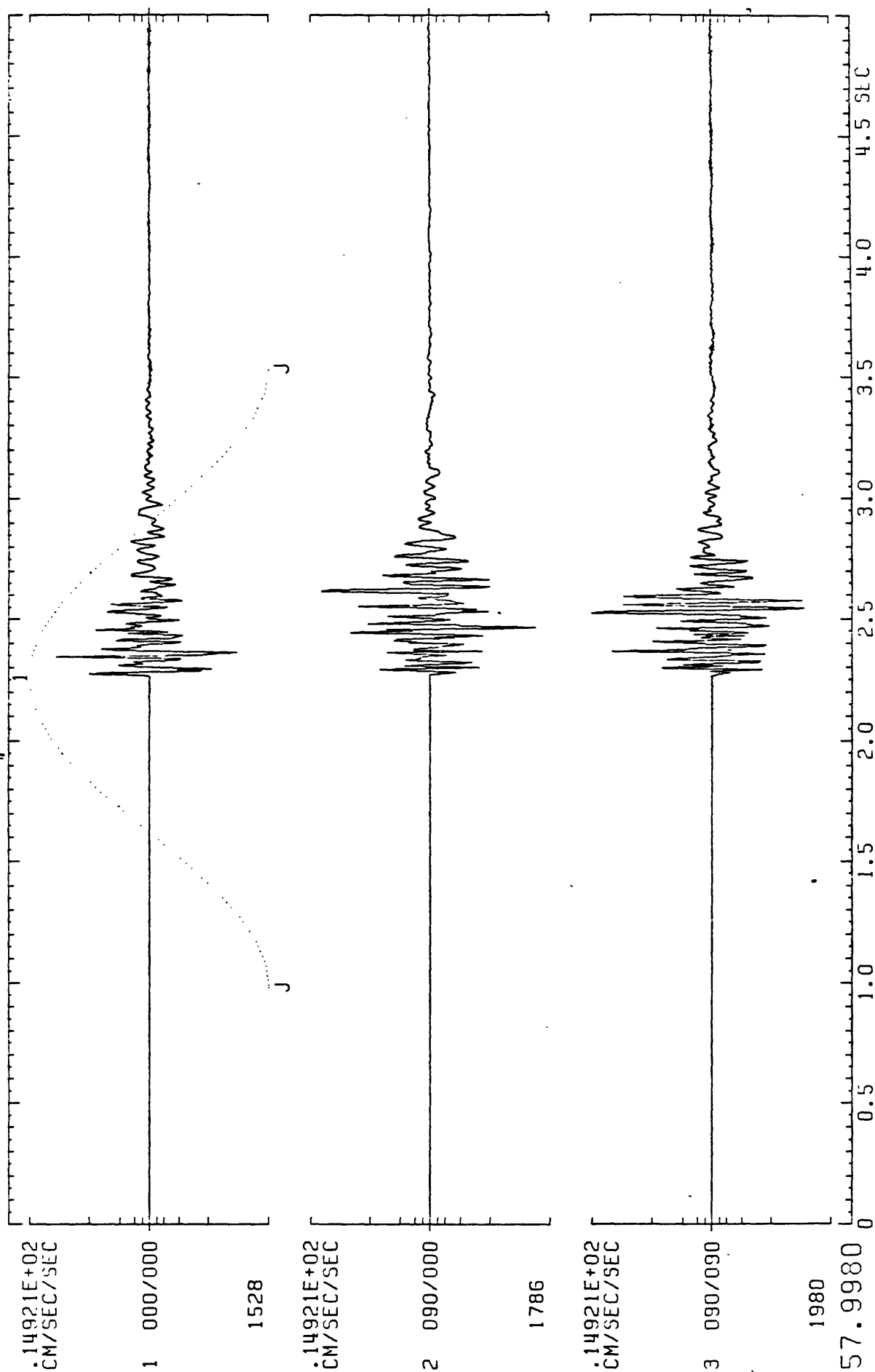


Figure 24

MOTION=ACCEL RAT S/S=200. SAM=01024 33019307A.C2C
 B=40 T=-40 L=+400
 M#1=[C1 000/000], 0000053, J"), DL=0, CB=1, HP=1, ED=A"

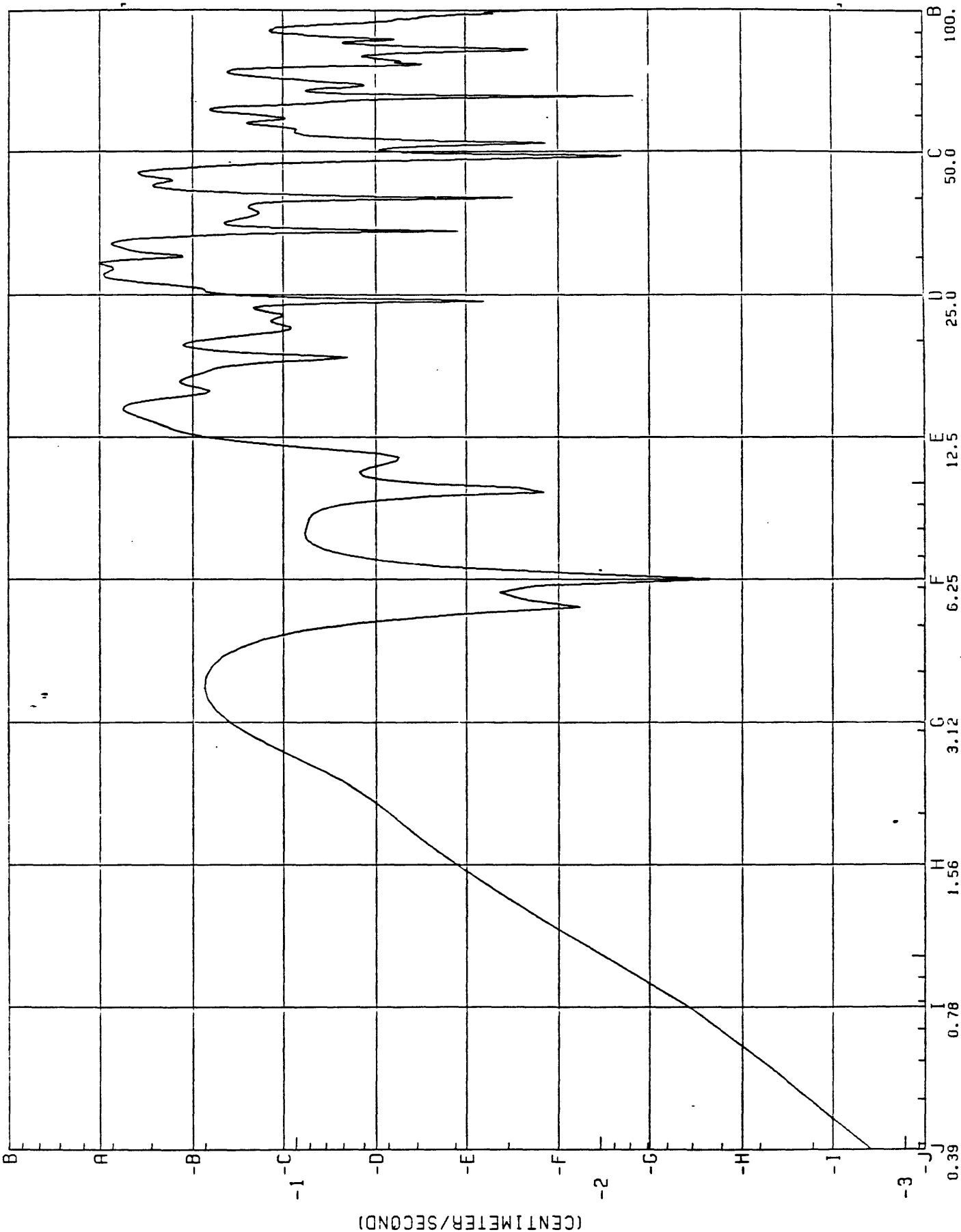


Figure 25

3301930TV.G2G

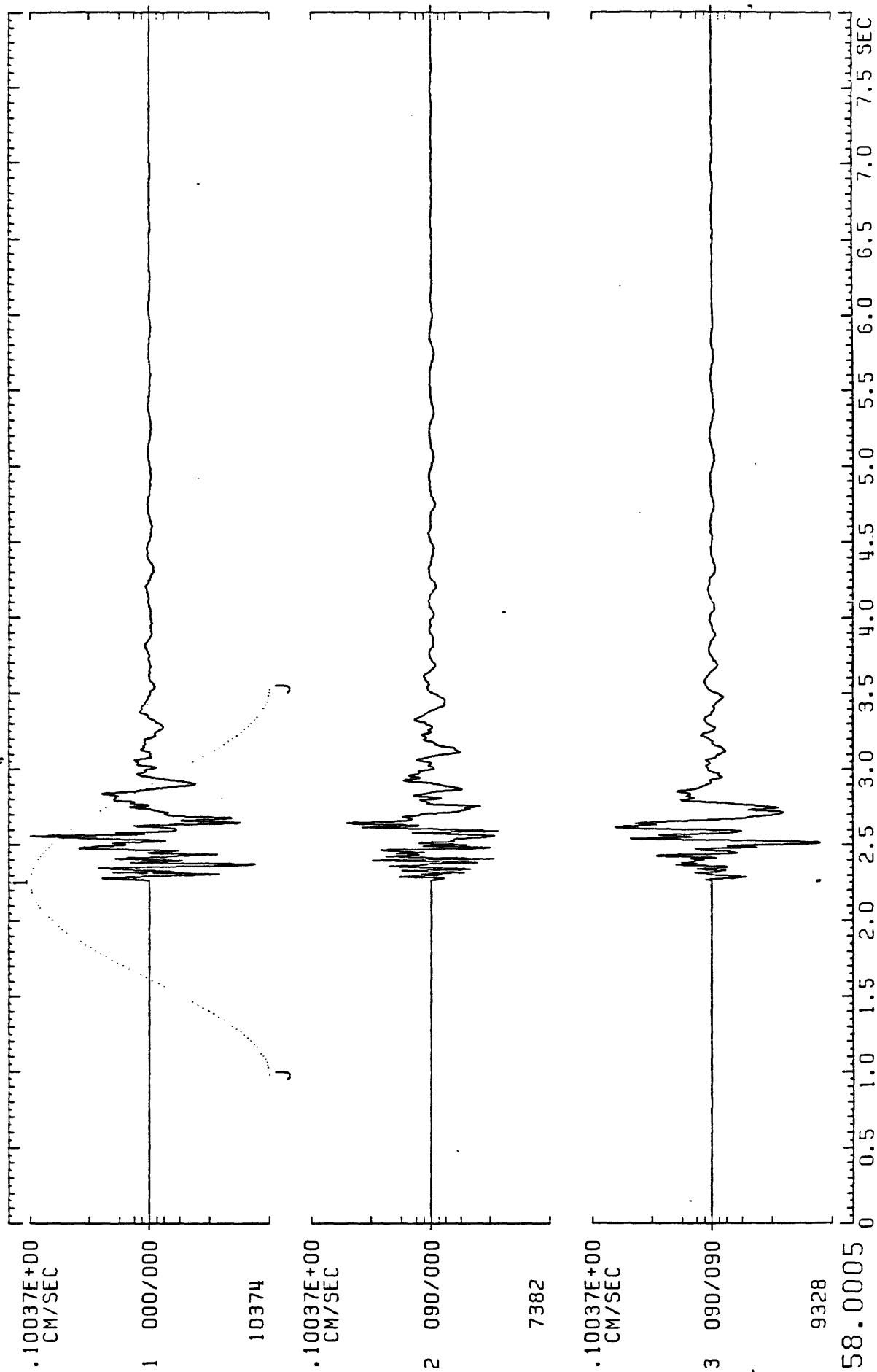


Figure 26

M*1=(C1 000/0007,0000052,J"),BL=0,CB=1,HP=1,ED=A"

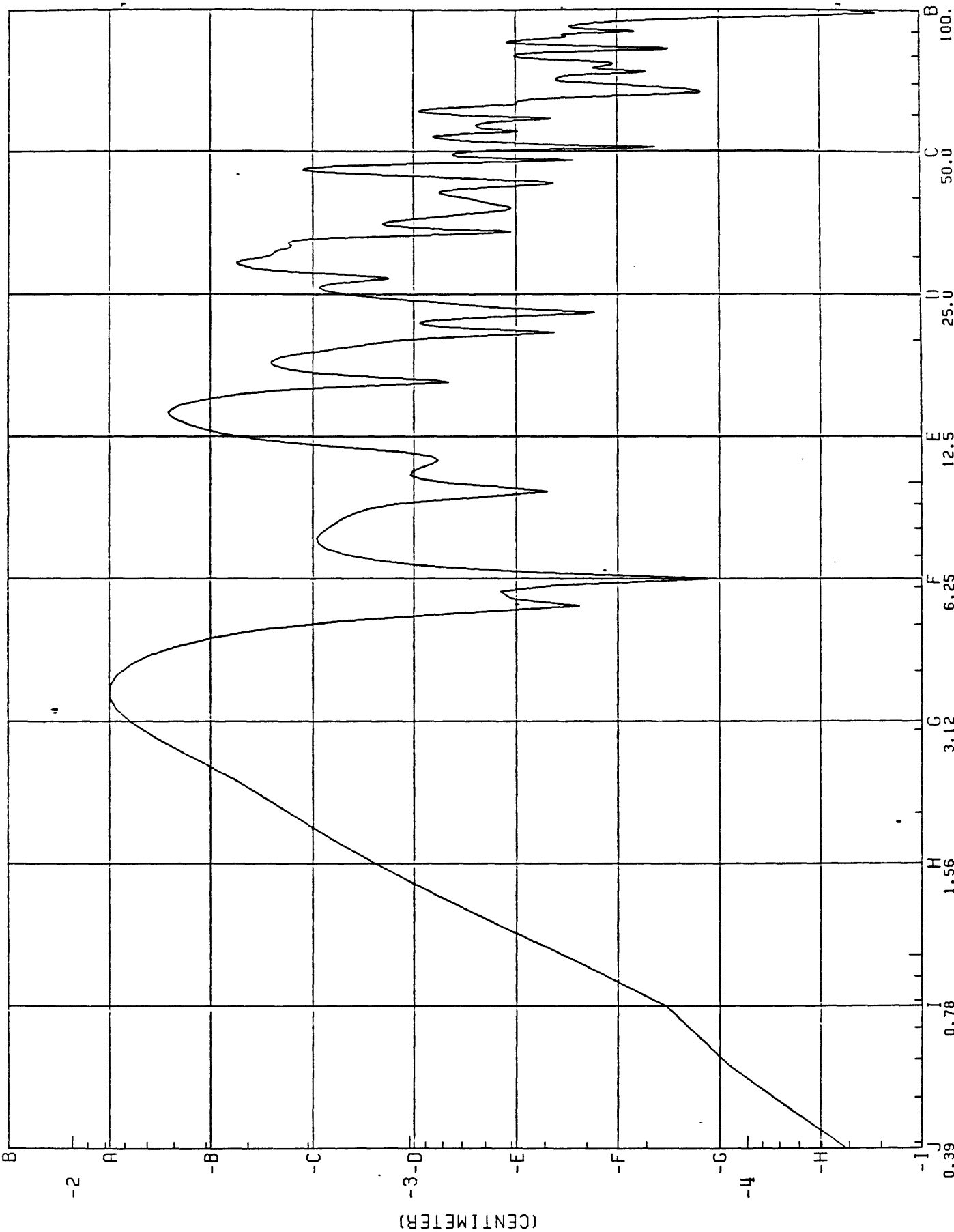


Figure 27

3301931AA.G3G

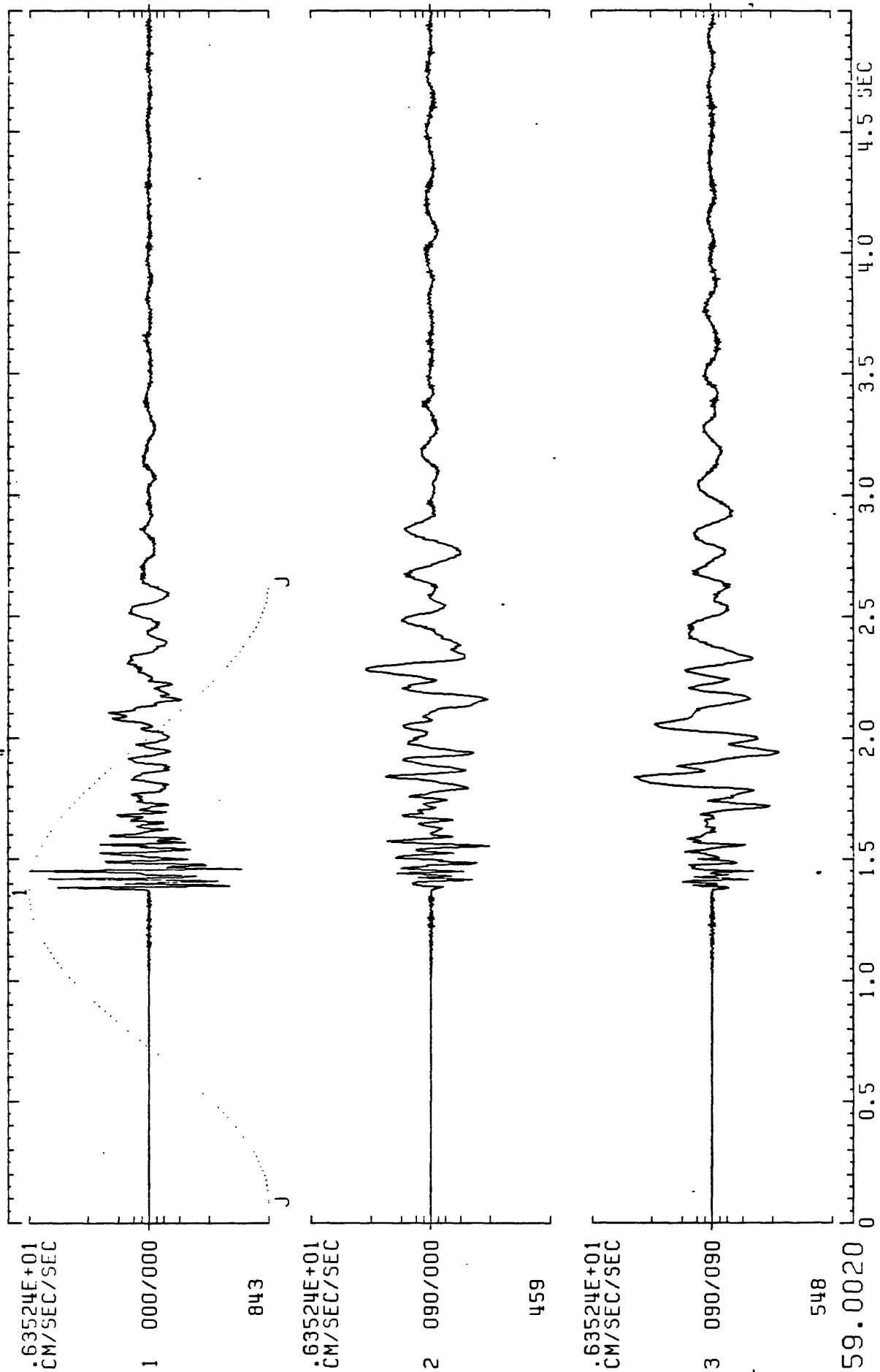


Figure 29

M*1=(C1 000/0000,00000074,J"),BL=0,CB=1,HP=1,ED=A"

MOTION=ACCEL RAT S/S=200. SAM=01024 3301931RA.636

B=20 T=-20 L=+200

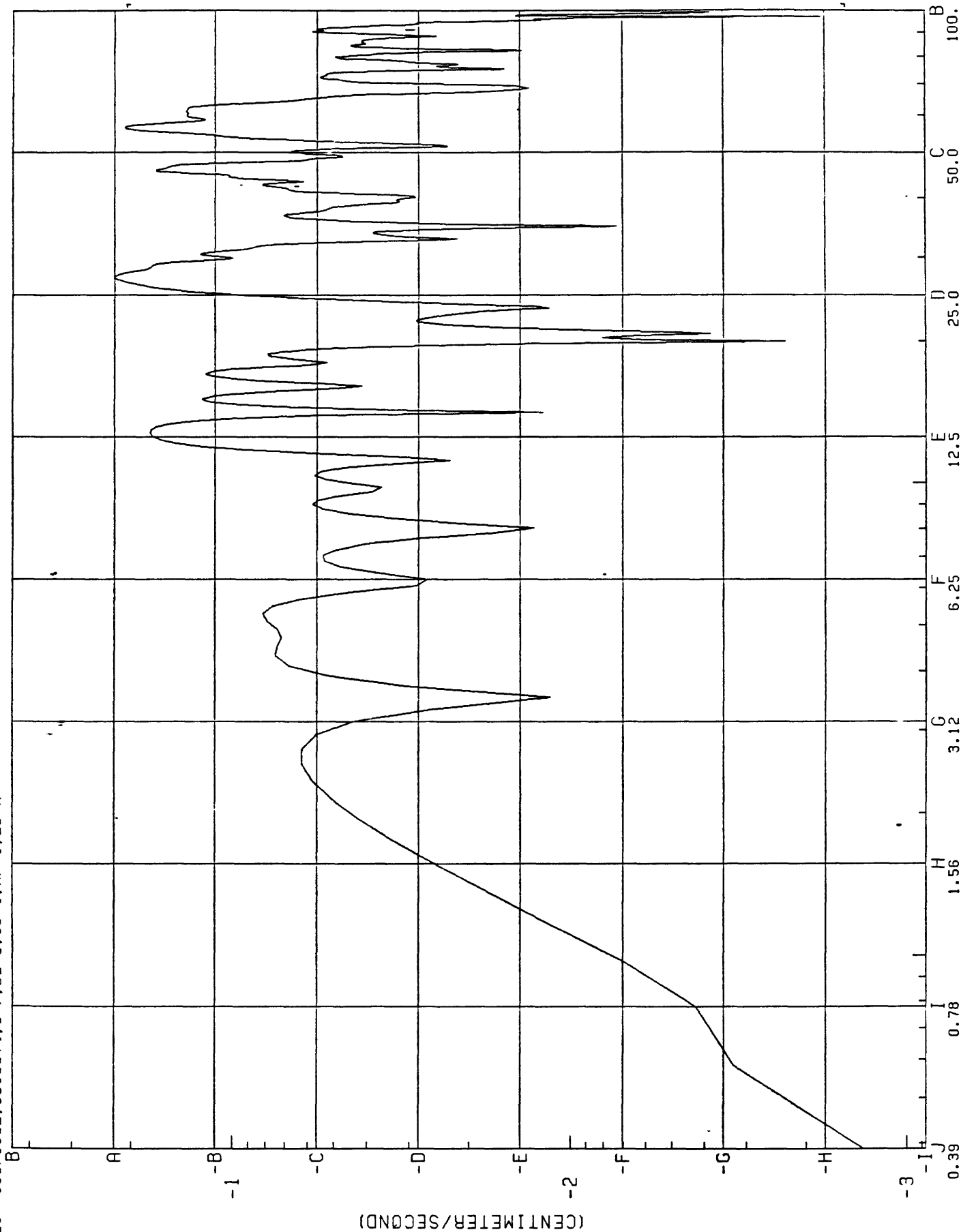


Figure 29

3301931AV.G3G

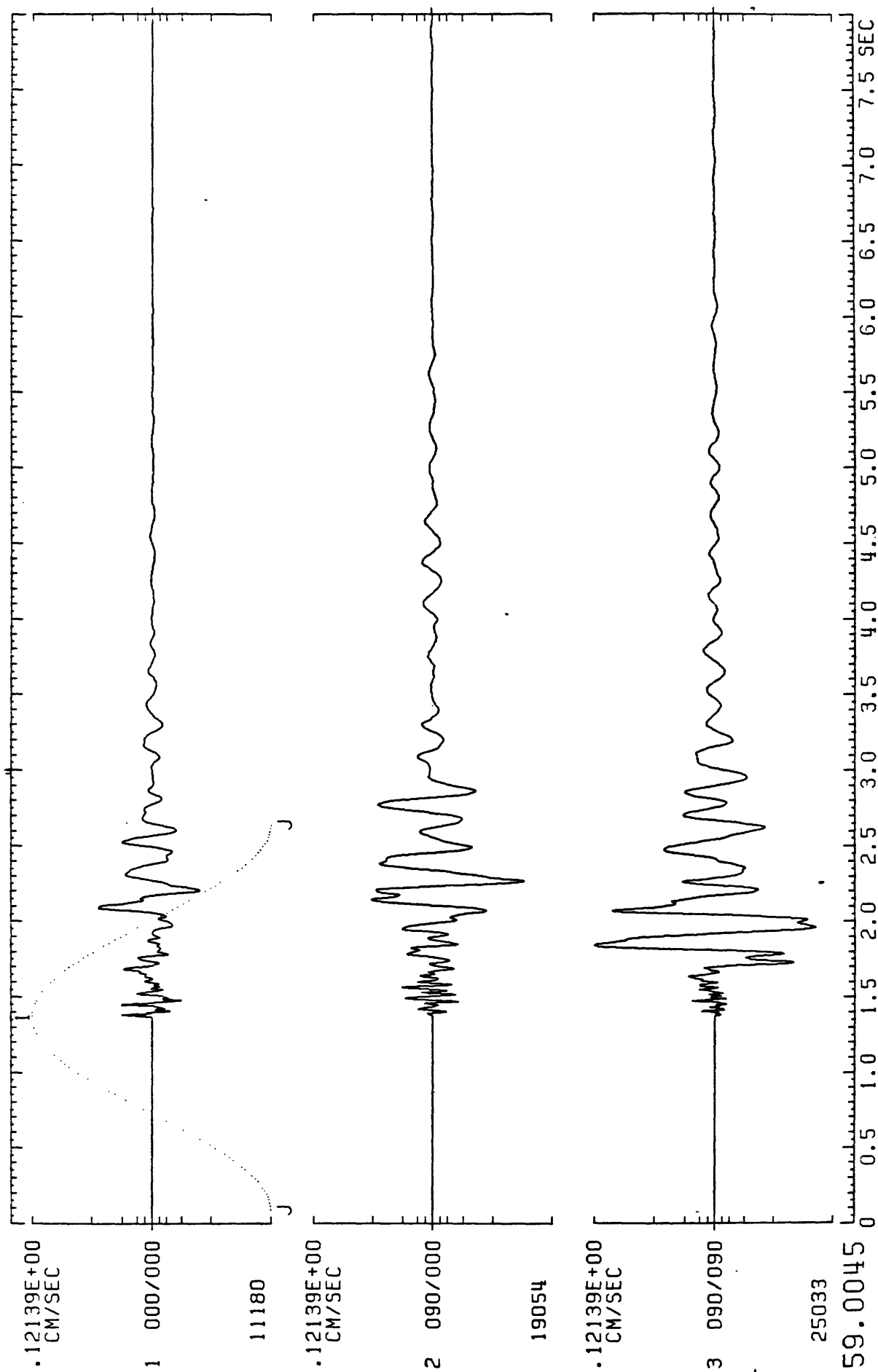
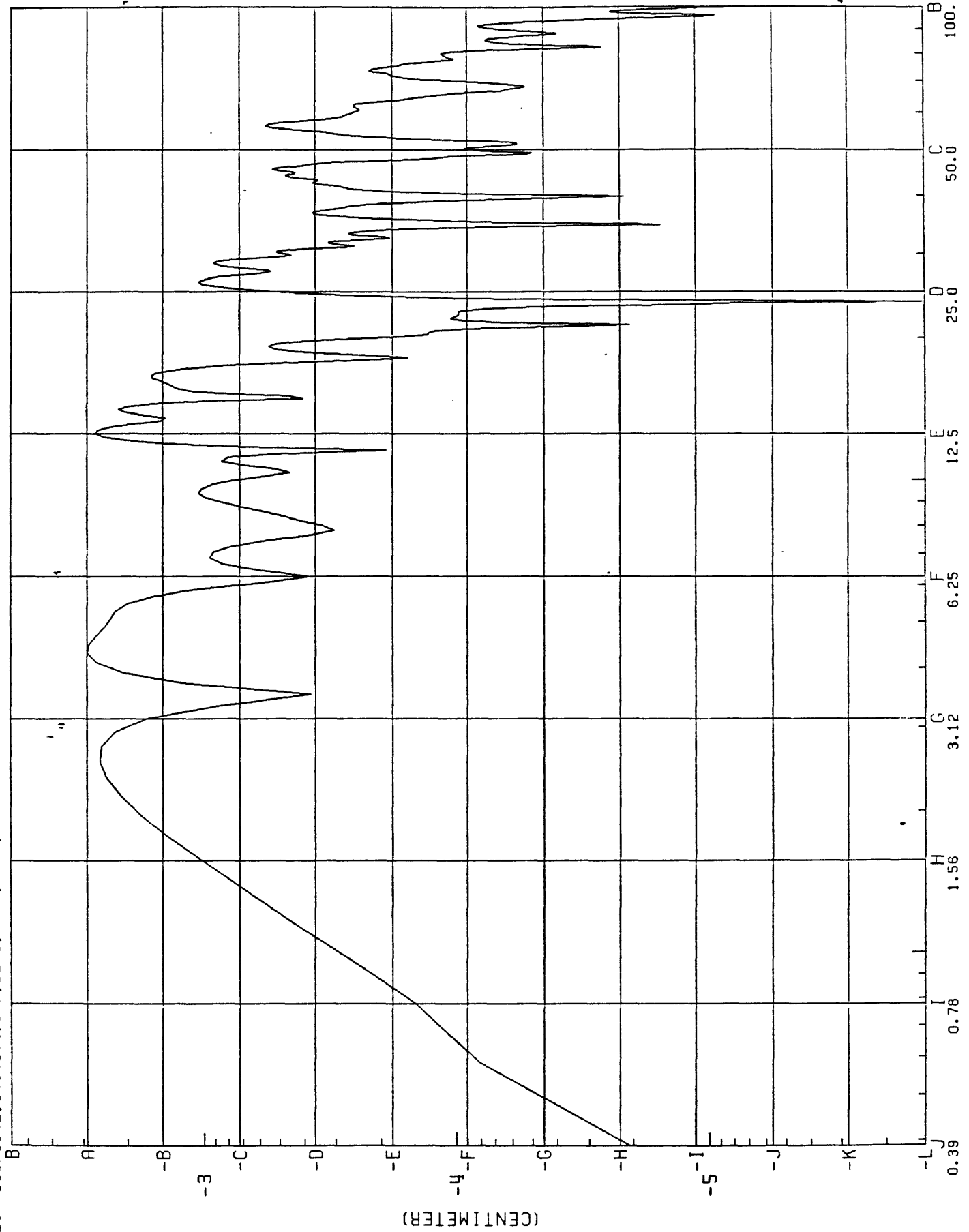


Figure 30

M*1=(C1 000/000J,0000074,J"),BL=0,CB=1,HP=1,ED=A"



MOTION=VELOCITY S/S=200. SAM=01024 3301931HV.03G
B=20 T=-20 L=+200

Figure 31

3301930TA.G4G

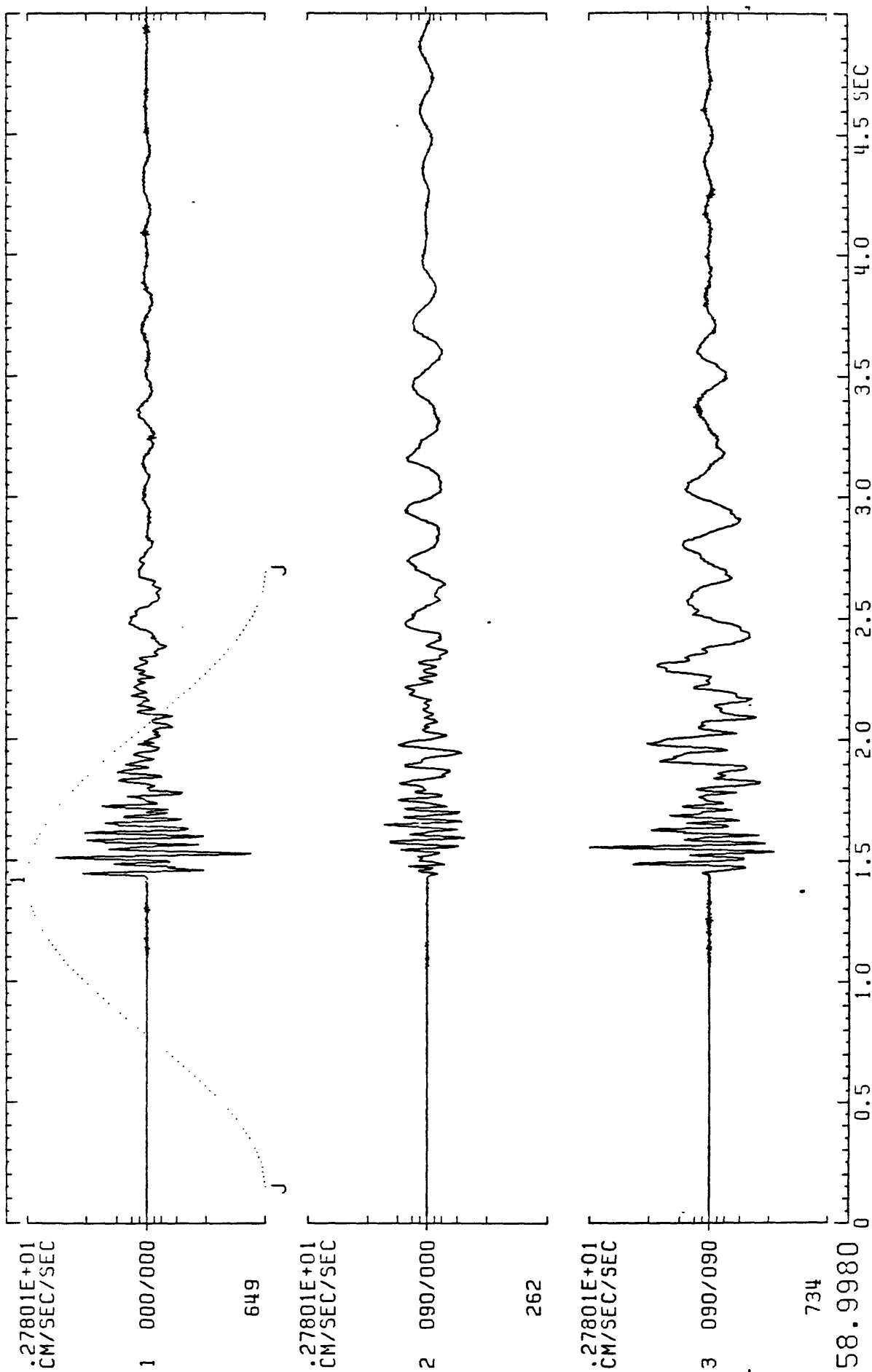


Figure 32

M*1=[C1 000/0003,0000085,J"),RL=0,CB=1,HP=1,ED=A"

MOTION=ACCEL RAT S/S=200. SAM=01024 33019301A.G4G

B=20 T=-20 L=+200

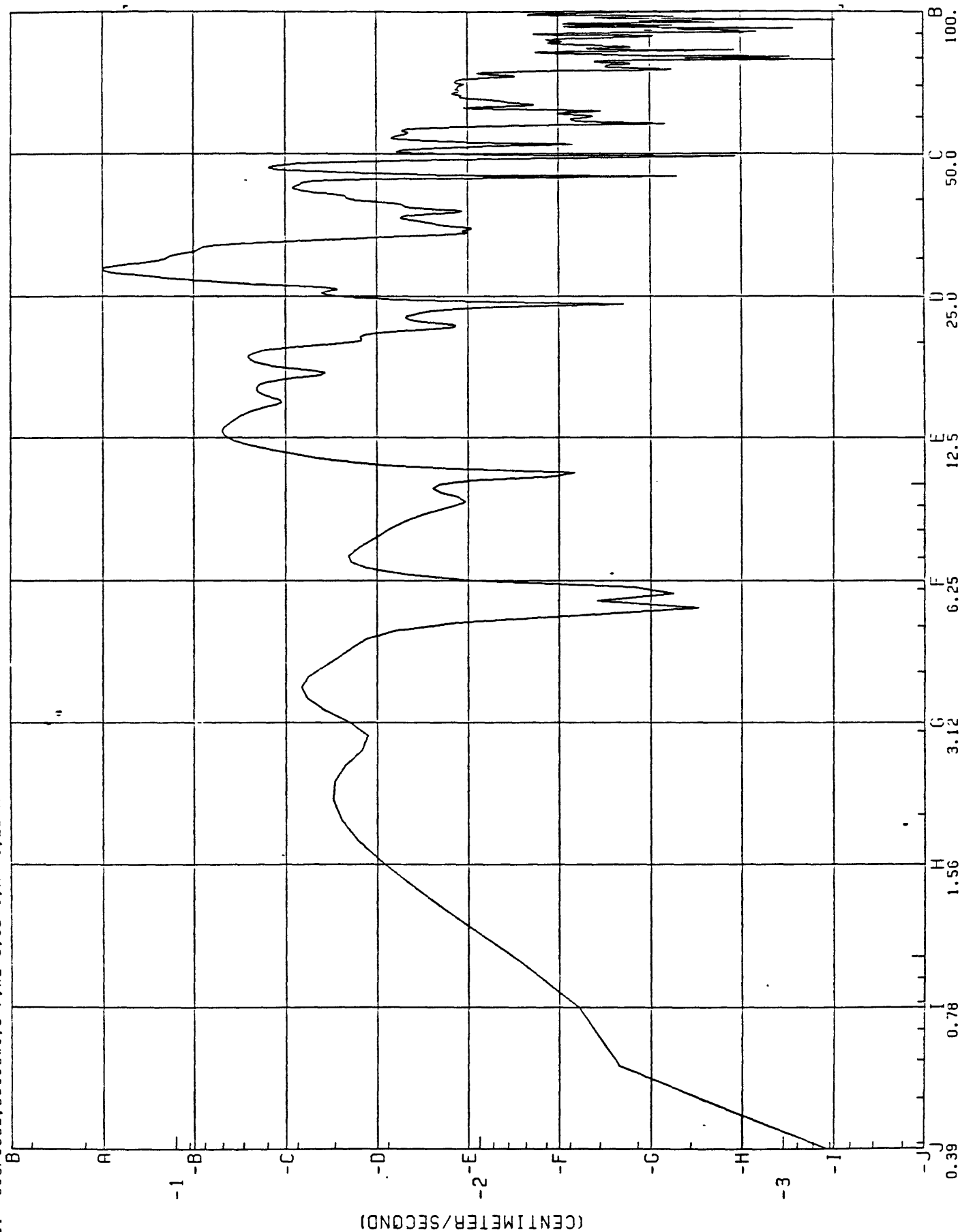


Figure 33

3301930TV.G4G

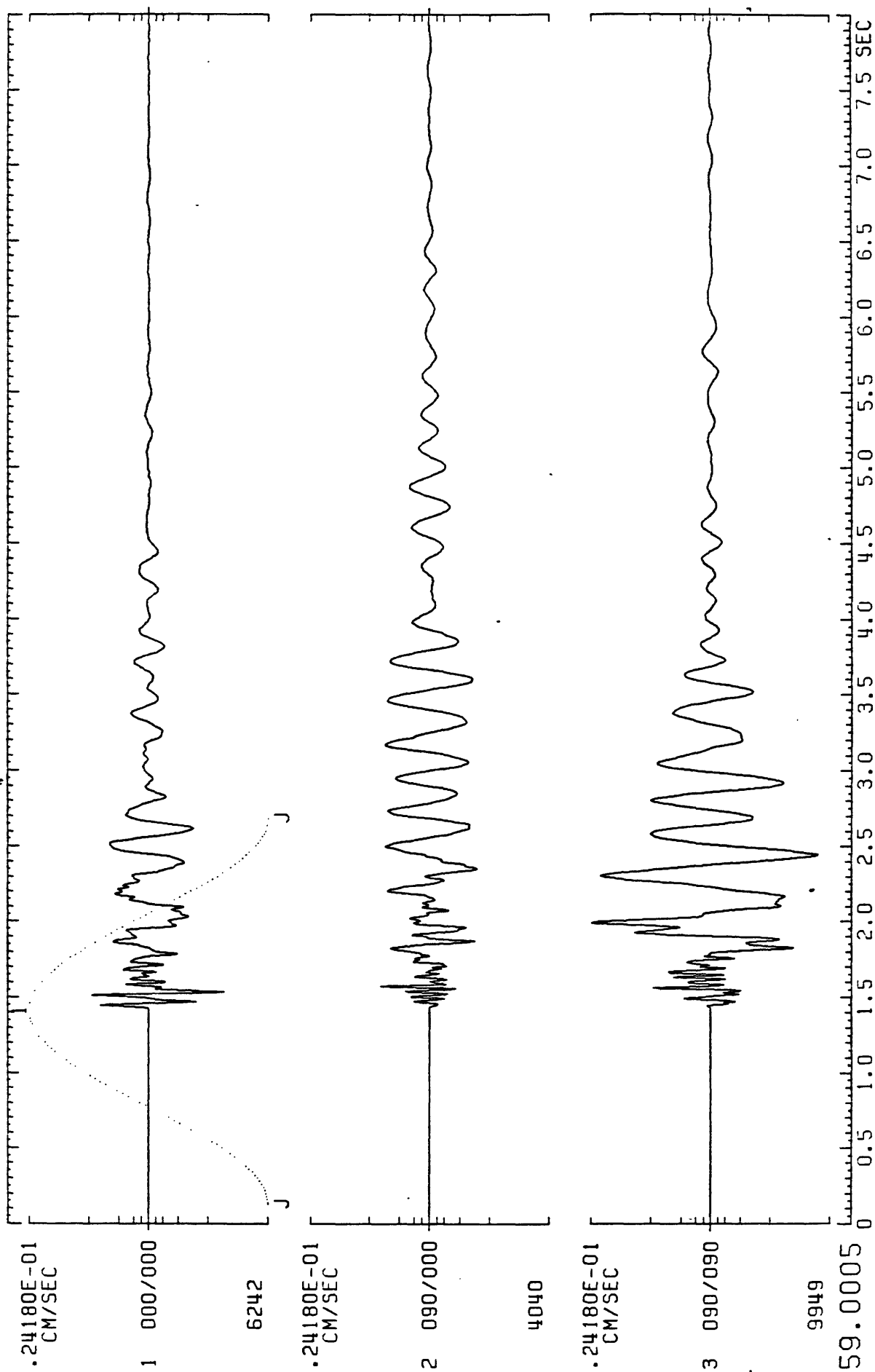


Figure 34

MOTION=VELOCITY S/S=200. SAM=01024 3301930TV.G4G

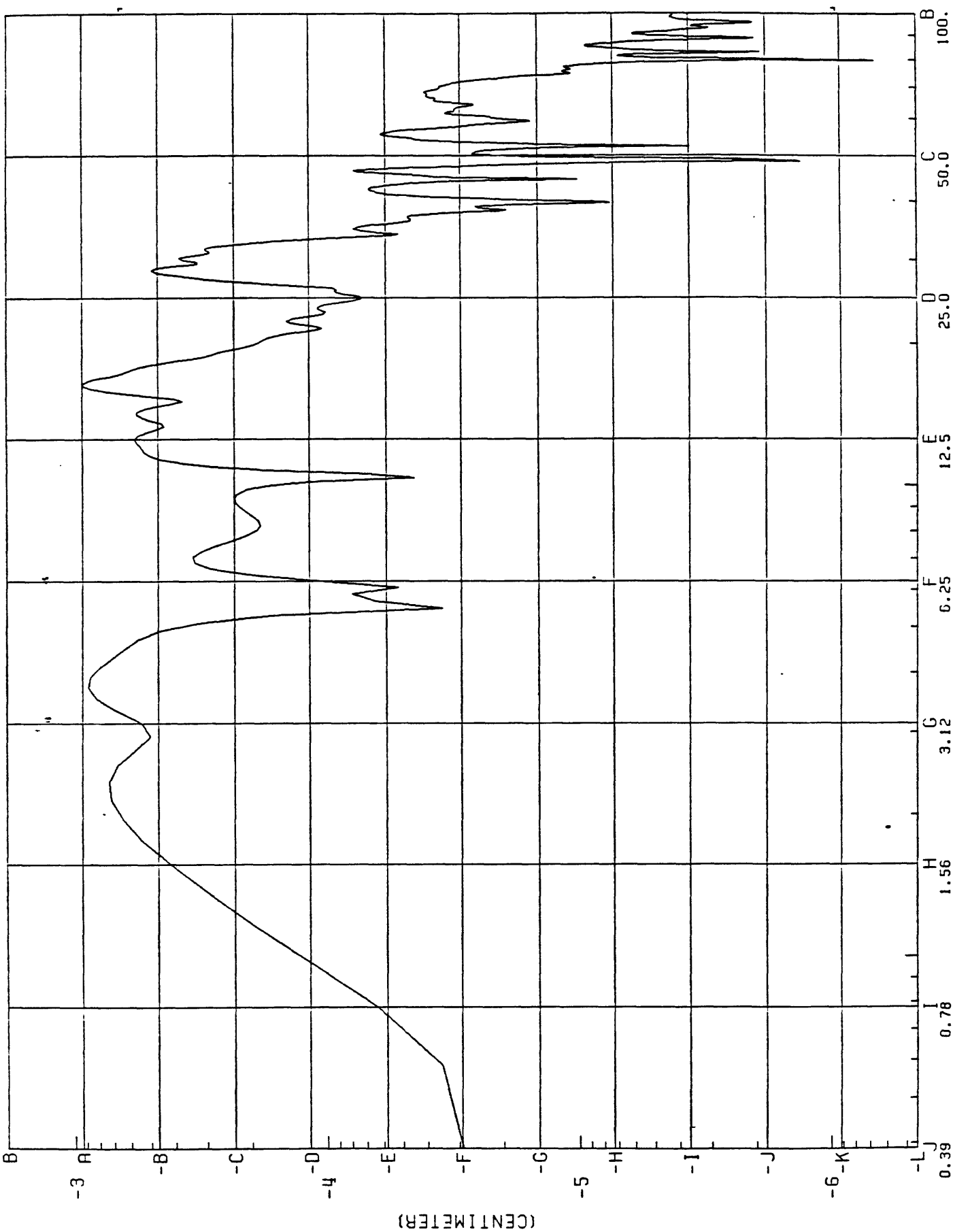


Figure 35

3301931AV.G5V

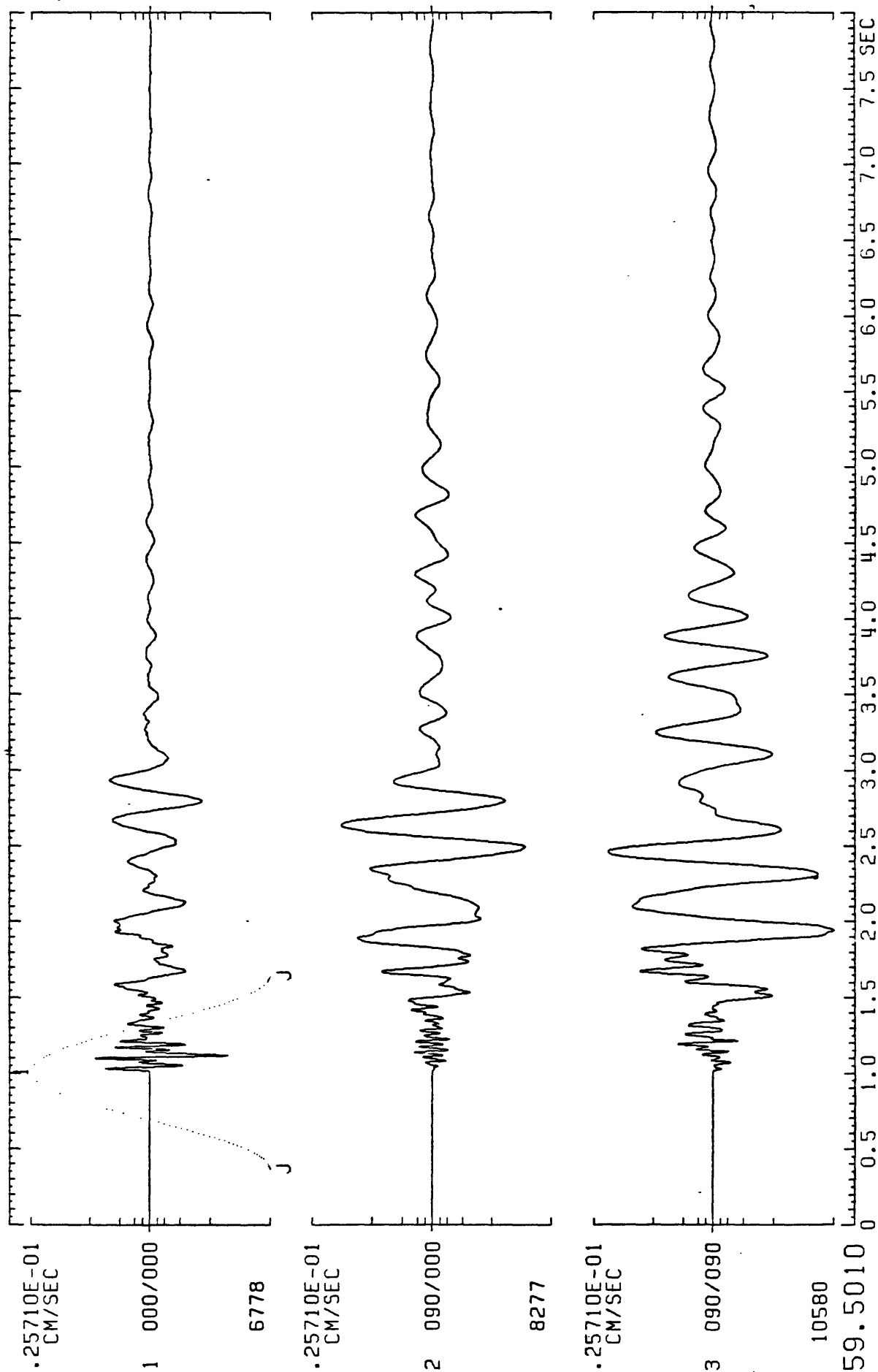


Figure 36

MOTION=VELOCITY S/S=400. SAM=01024 3301931HV.GSV

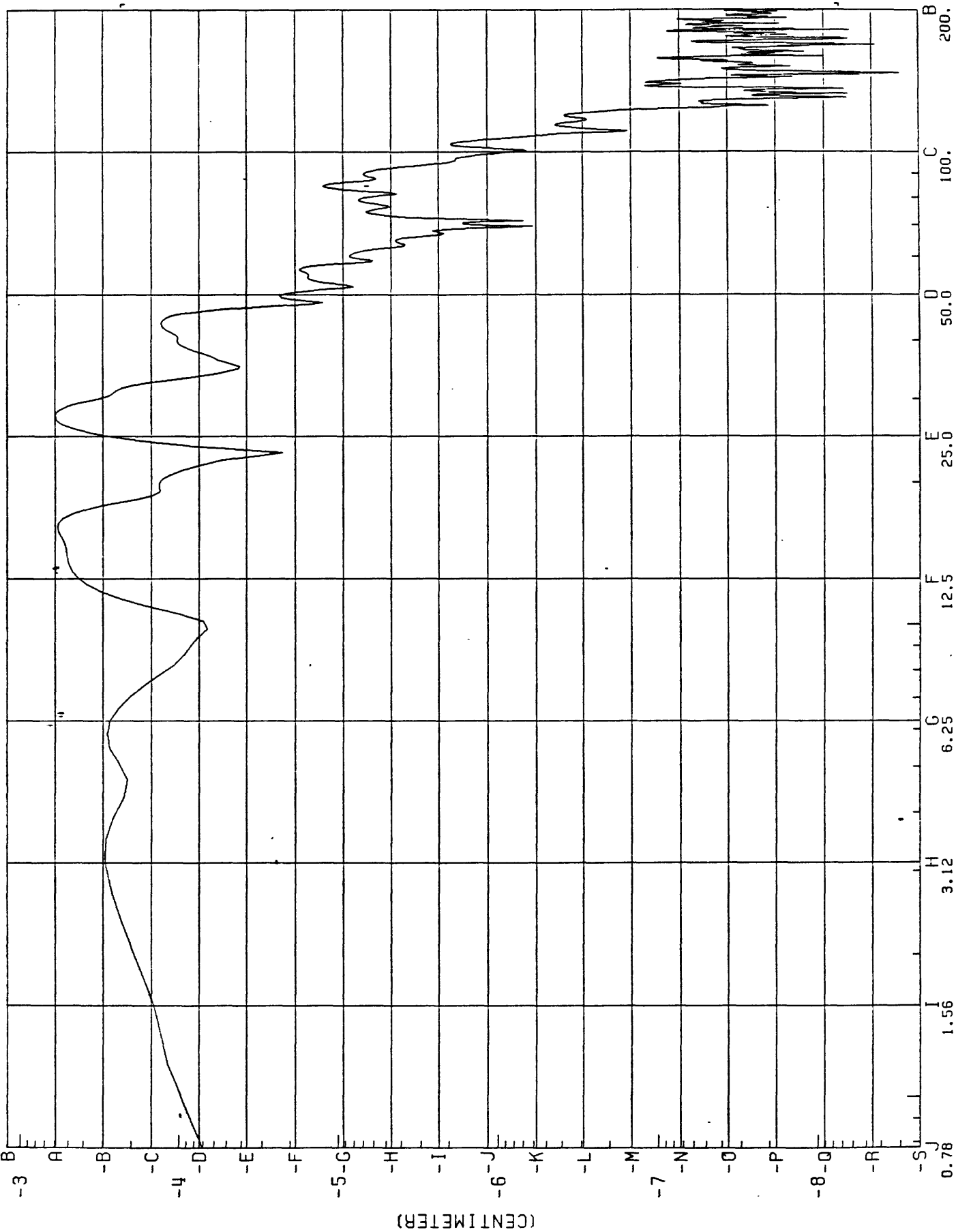


Figure 37

3301931AV.C6V

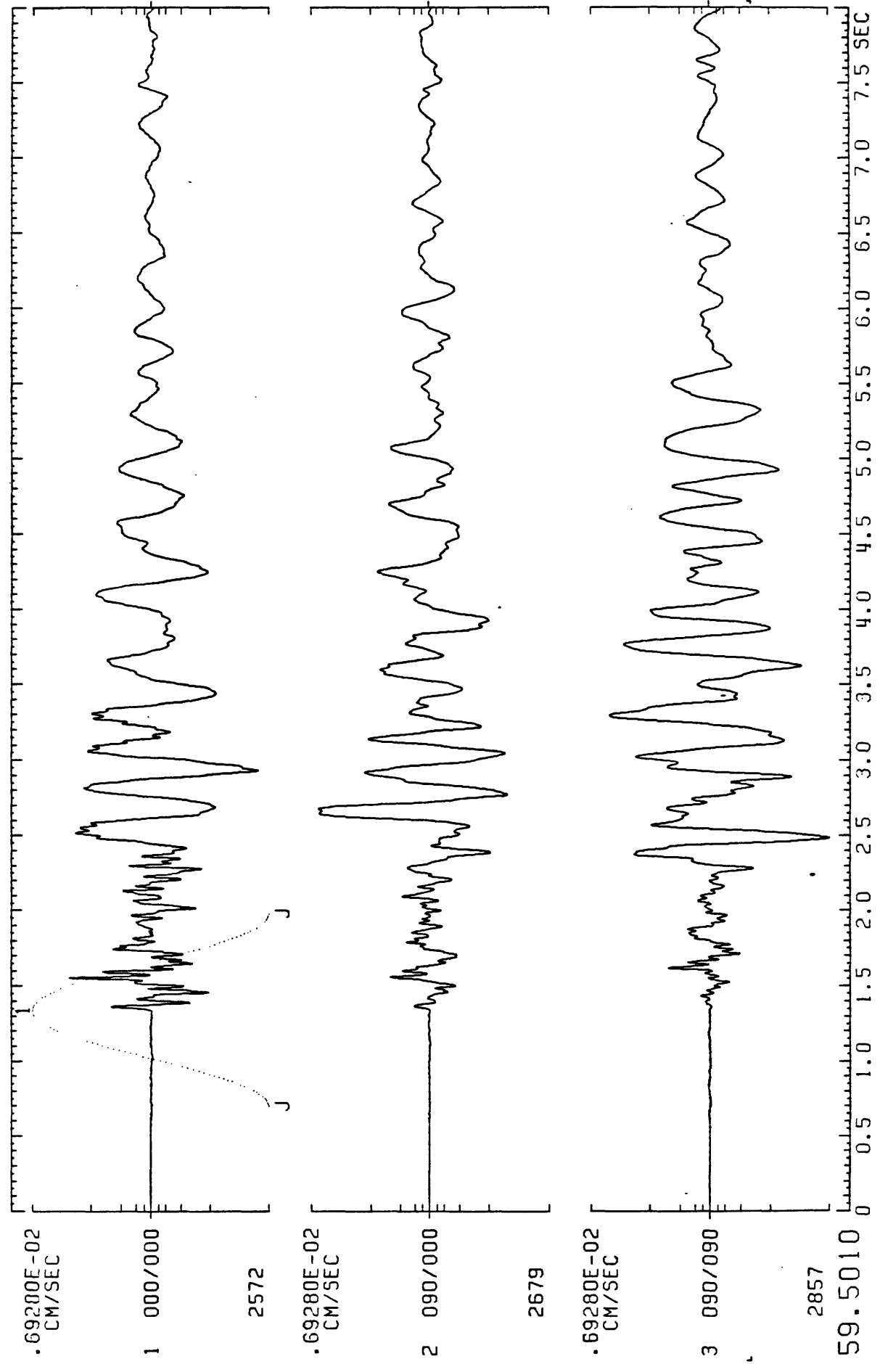


Figure 38

M*1=(C1 000/000J,0000336,J"),BL=0,CB=1,HP=1,ED=A"

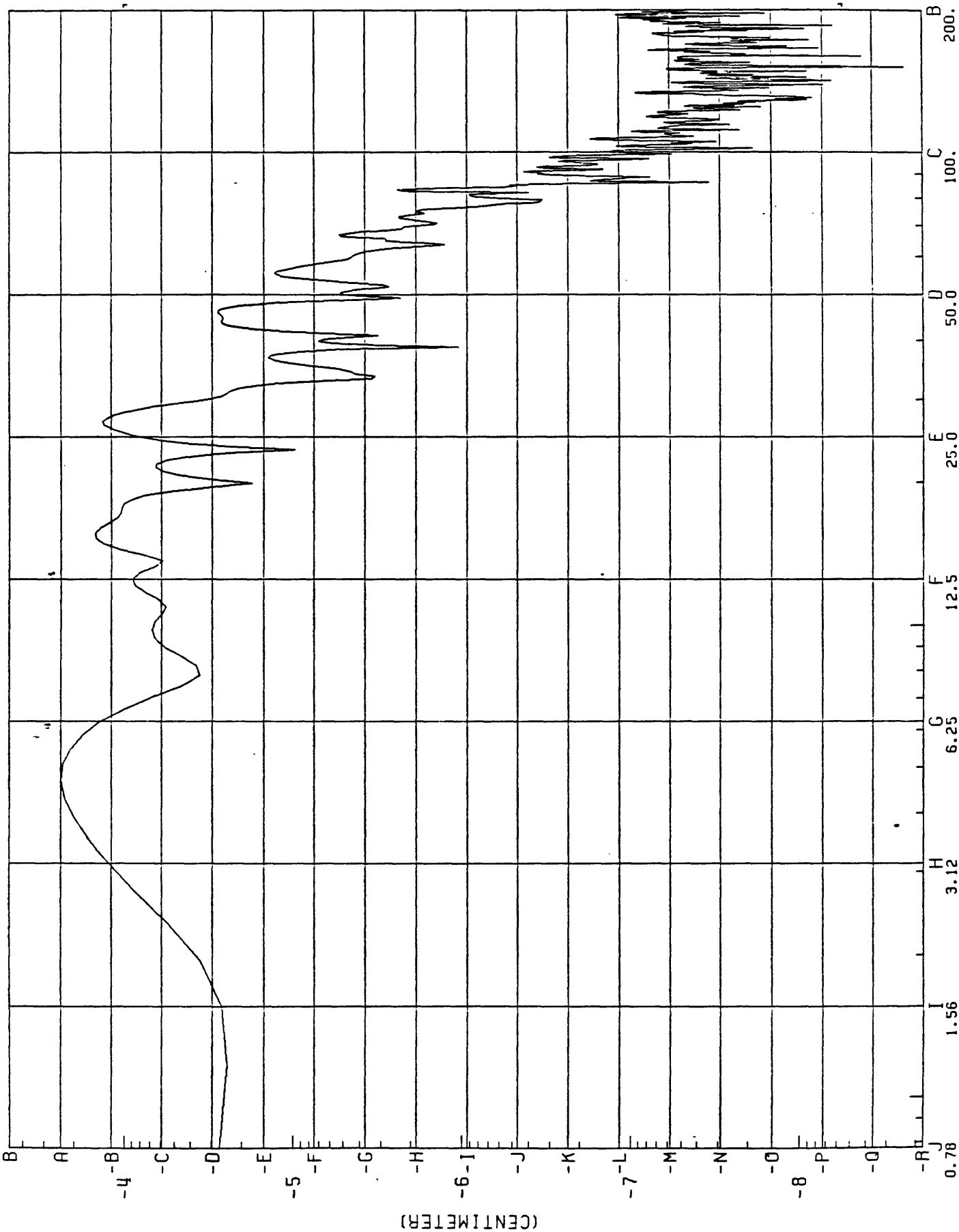


Figure 39

M*1>1__000/000>186J>B0C1A1F1E0>R<3261929TV.66V>W*1>1__000/000>379J>B1C1A1F1E0>

MOTION=VELOCITY S/S=200. SAM=01024 3261929TV.62G

B=20 T=-20 L=+200

RATIO AMPLITUDE

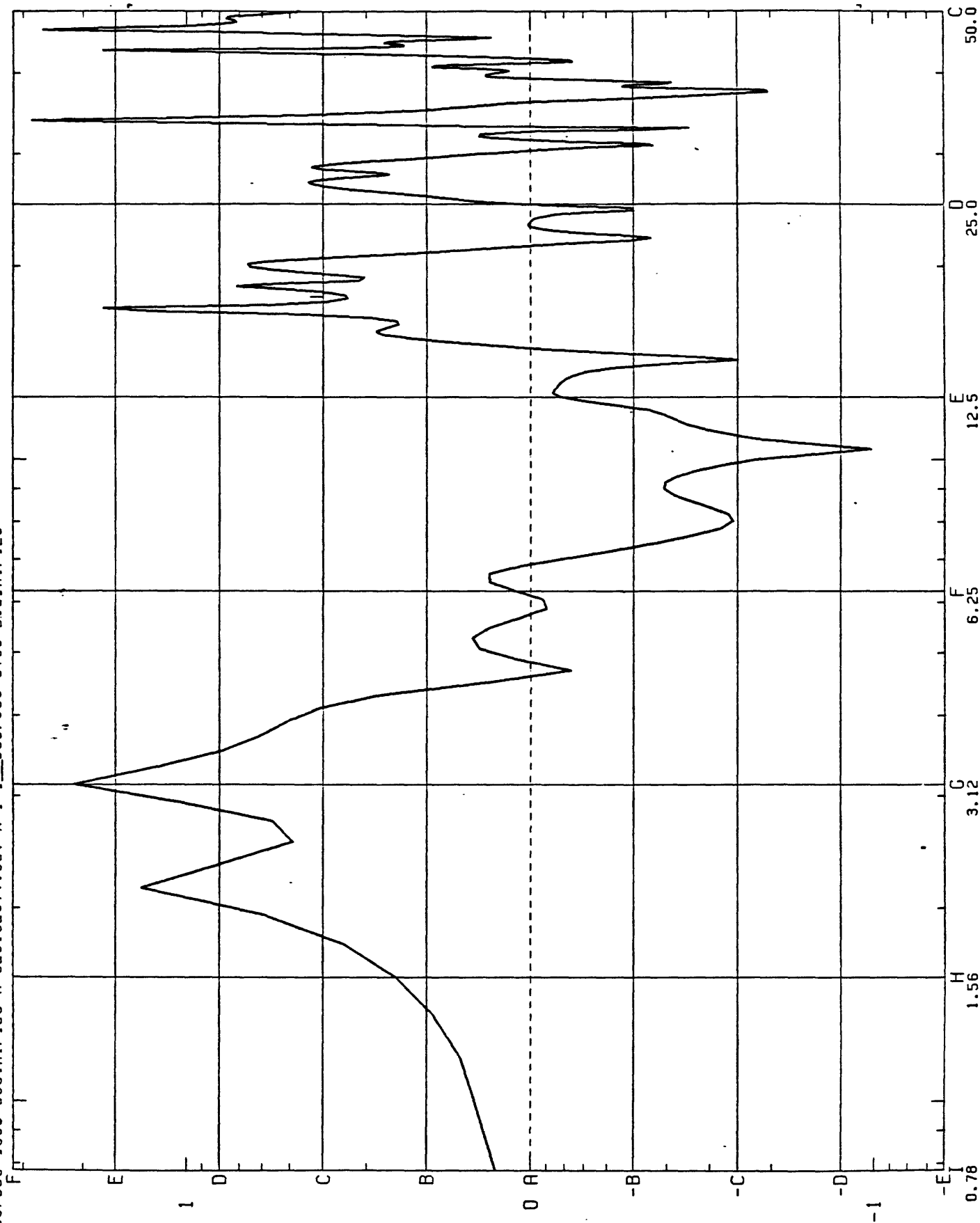


Figure 40

MOTION=VELOCITY S/S=200. SAM=01024 3301930TV.G2G

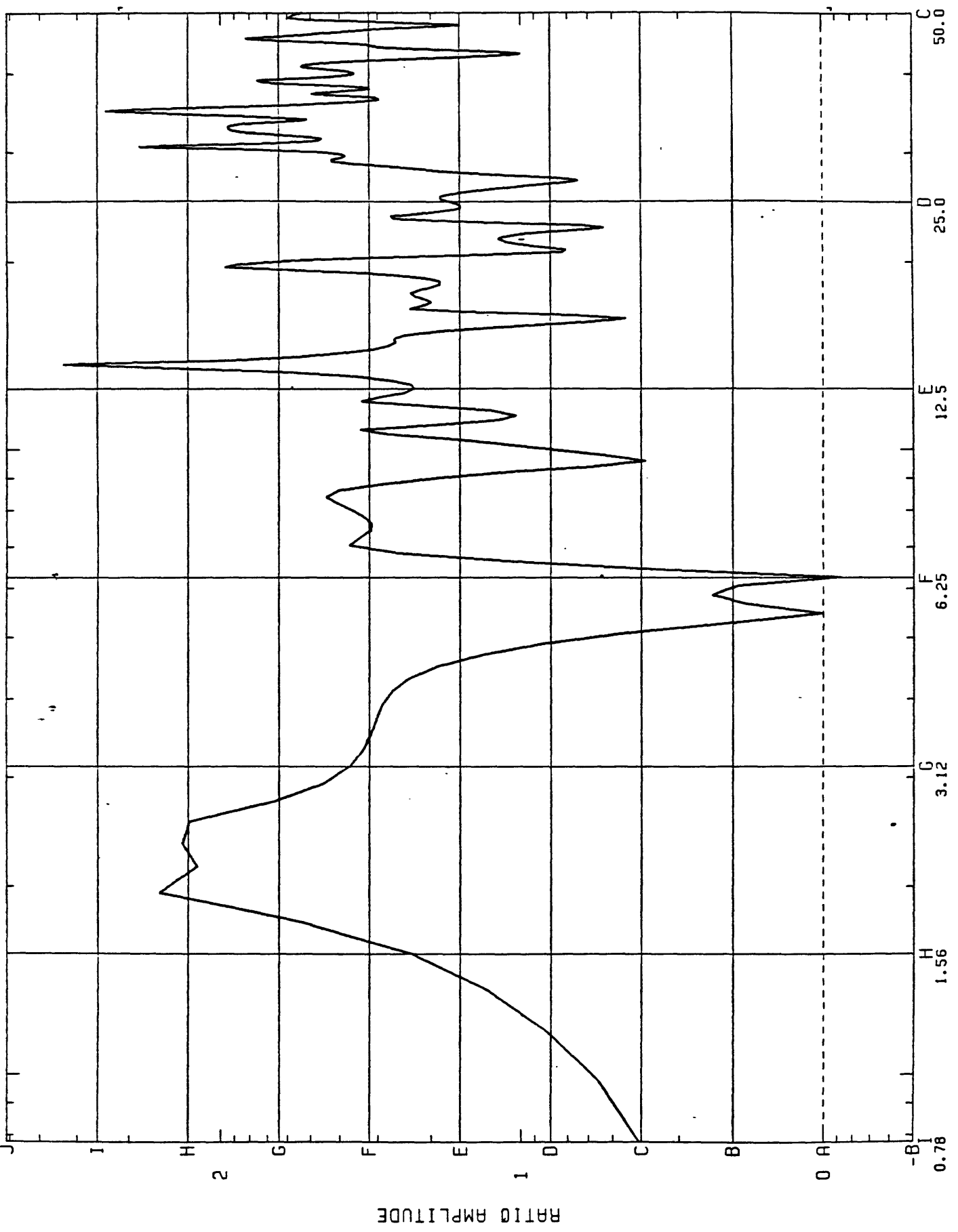


Figure 41